 doi:10.20944/preprints202104.0052.v1

System of Time Fractional Models for COVID-19: Modeling, Analysis and Solutions

Olaniyi Iyiola[1], Bismark Oduro[2], Trevor Zabilowicz[3], Bose Iyiola[4], and Daniel Kenes[5]

[1,2,4,5]Department of Mathematics and Physical Sciences, California University of Pennsylvania, California, PA, USA.
[3]Department of Computer Science, Information Systems, and Engineering Technology, California University of Pennsylvania, California, PA, USA.
[1]iyiola@calu.edu & niyi4oau@gmail.com
[2]oduro@calu.edu
[3]zab5682@calu.edu
[4]iyi8607@calu.edu
[5]ken6393@calu.edu

Abstract

The emergence of the COVID-19 outbreak has caused a pandemic situation in over 210 countries. Controlling the spread of this disease has proven difficult despite several resources employed. Millions of hospitalization and deaths have been observed, and thousands of cases daily with many measures in place. Due to the complex nature of COVID-19, we proposed a system of time-fractional equations to understand the transmission of the disease better. Nonlocality involved in the model has made fractional differential equations appropriate for modeling the behavior. However, solving these types of models is computationally demanding. Our proposed generalized compartmental COVID-19 model incorporates effective contact rate, transition rate (from exposed quarantine and recovered to susceptible and infected quarantined individuals), quarantine rate, disease-induced death rate, natural death rate, natural recovery rate, recovery rate of quarantine infected for a holistic study of the coronavirus disease. A detailed analysis of the proposed model is carried out, including the existence and uniqueness of solutions, local and global stability analysis of the disease-free equilibrium analysis, and sensitivity analysis. Furthermore, numerical solutions of the proposed model are obtained with the generalized Adam-Bashforth-Moulton method developed for the fractional order model. Our analysis and solutions profile show that each of these incorporated parameters is very important in controlling the spread of COVID-19, especially quarantining exposed and infected individuals and the effective contact rate. Based on the results with different fractional order, we observe that there seems to be a third or even fourth wave of the spike in cases of COVID-19, which is what is happening right now in many countries.

Keyword: Coronavirus; COVID-19; Diseases Modeling; time-fractional,quarantine.

1 Introduction

The emergence of the COVID-19 outbreak has caused a pandemic situation in over 213 countries. The Coronavirus disease, formally known as COVID-19 or SARS-CoV-2, originated in the city of Wuhan, in the Hubei province of China. The source is still unknown. It is believed that the appearance of the virus in the human population was caused by an animal reservoir. In recent times, many countries have started an investigation into the exact source of this new coronavirus. COVID-19 has spawned a global pandemic that has substantially affected millions around the world. The Coronavirus disease causes an upper-respiratory infection that is easily transmitted between hosts with no known vaccine. The Centers for Disease Control and Prevention have declared this outbreak a public health risk. This disease spreads through droplets caused by coughs, sneezes, or talking within a range of approximately six feet. It is known that social distancing and face masks are effective ways to prevent the spread of the virus between hosts. COVID-19 has affected people all over the world and continues to spread. Throughout history, major pandemics have occurred, such as the Spanish Flu (1981 – 1920) and the recent Ebola epidemic (2014 – 2016), that have had a major impact on human health and global economics. As for recently (March 2021), the coronavirus has infected more than 127.3 million people worldwide, killing over 2.7 million people. Specifically, in the USA, over 31 million cases already recorded with over 540,000 deaths [1].

The importance of modeling and tracking the severity of the virus is not only necessary to prepare for future outbreaks but to inform governments and citizens of what they should be doing now to mitigate transmission and infection. By modeling and tracking the trend of the current outbreak, we can prepare for outbreaks in the upcoming seasons. Doing this will help reduce the severity of following Coronavirus outbreaks. There have been many proposed mathematical models and analysis by a large number of infectious disease researchers on COVID-19, and similar diseases see [2, 3, 4, 5, 6, 7, 8, 9, 10, 11]. However, COVID-19 is rare, complex and many things are yet unknown, which set limitations to what known models could capture. Nearly every phenomenon in many fields of Science, Engineering, and Social Science can be alternately modeled using non-integer (fractional) order derivatives. This is due to the non-locality property, which is intrinsic to many complex systems. These applications are widely seen as modeling tools in many areas such as biological modeling, viscoelasticity, control theory of dynamical systems, nanotechnology, anomalous transport, and anomalous diffusion, financial modeling, and random walk [12, 13, 14, 15, 16, 17, 18, 19, 20, 21, 22]. It should be noted here that solving fractional differential equations is very difficult due to the memory effect. Beyond numerical methods, which often time are computationally demanding, different analytical methods have been proposed to handle linear and nonlinear fractional differential equations, see [23, 24, 25, 26, 27, 28, 13, 29, 30].

Due to the complex nature of COVID-19, this paper explores the use of fractional calculus to develop mathematical models in order to understand and answer the following pertinent questions: (1) what parameters are essential (most impactful) for control measure purposes (2) dynamics of the spread and long time impact of the disease in different popu-

Preprints (www.preprints.org) | NOT PEER-REVIEWED | Posted: 2 April 2021 doi:10.20944/preprints202104.0052.v1

lation densities (3) what to expect at the resurgence of the outbreak and necessary control measure to reduce the impact. This work is focused on advancing research to understand better factors that could help curtailing or possible control measures for eradication for a long time benefit. Different control measures are investigated using effective, efficient, and more general mathematical models to reveal the intrinsic nature of the COVID-19. Modeling, analysis, and numerical solutions are the focus of the current paper on the disease transmission and spread that includes understanding the delay to 'flattening the curve' as experienced in many cities and countries.

Specifically, our proposed generalized compartmental COVID-19 model takes into account many key parameters to gain insight into the complexity of the disease. The parameters considered are effective contact rate, transition rate (from exposed quarantine and recovered to susceptible and infected quarantined individuals), quarantine rate, disease-induced death rate, natural death rate, natural recovery rate, and recovery rate of quarantine infected. We simulate and discuss the parameters on the dynamics of the solution profiles. In this paper, a detailed analysis of the proposed model is carried out, including the existence and uniqueness of solutions, local and global stability analysis, endemic equilibrium analysis, and sensitivity analysis. In addition, numerical solutions of the proposed fractional SEQIR model are obtained using the generalized Adam-Bashforth-Moulton method developed for the fractional order model.

The rest of the paper is structured as follows: In Section 2, preliminaries are presented to include basic definitions, notations used in this present investigation, and useful results from the literature. The generalized mathematical model is formulated in Section 3, which accounts for the loss of immunity of the infected recovered individuals. Analysis of the model to include the existence and uniqueness of solutions, local and global stability analysis, endemic equilibrium analysis, and sensitivity analysis is presented with detailed proofs in Section 4. The numerical simulation of the proposed model is presented in Section 5. Finally, Section 6 is devoted to summary and recommendations.

2 Preliminaries

In this section, we present some definitions, notations and some known results needed in sequel. Caputo's fractional derivative is adopted in this work.

Definition 2.1 *A real valued function u is said to be in the space C_η, $\eta \in \mathbb{R}$, $t > 0$, if there exists a real number p with $p > \eta$ such that*

$$u(t) = t^p g(t),$$

where $g \in C[0, \infty)$ and it is said to be in the space C_η^m iff $u^{(m)} \in C_\eta$, $m \in \mathbb{N}$.

Definition 2.2 *The Laplace transform is defined by*

$$\mathcal{N}(s) = \mathcal{L}\left(N(t)\right)(s) = \int_0^\infty e^{-st} N(t) dt, \tag{1}$$

where $N(t)$ is n-dimensional vector-valued function.

Preprints (www.preprints.org) | NOT PEER-REVIEWED | Posted: 2 April 2021 doi:10.20944/preprints202104.0052.v1

Definition 2.3 *The Riemann-Liouville's (RL) fractional integral operator of order $\alpha \geq 0$, of a function $u \in L^1(a,b)$ is given as*

$$J^{\alpha}u(t) = \frac{1}{\Gamma(\alpha)}\int_0^t (t-\tau)^{\alpha-1}u(\tau)d\tau, \quad t>0, \quad \alpha>0, \tag{2}$$

where Γ is the Gamma function and $J^0u(t) = f(t)$.

Definition 2.4 *The fractional derivative in the Caputo's sense is defined as [31],*

$$\mathcal{D}^{\alpha}u(t) = J^{n-\alpha}D^n u(t) = \frac{1}{\Gamma(n-\alpha)}\int_0^t (t-\tau)^{n-\alpha-1}u^{(n)}(\tau)d\tau, \tag{3}$$

where $n-1 < \alpha \leq n$, $n \in \mathbb{N}$, $t>0$.

Lemma 2.1 *Let $t \in (a,b]$. Then*

$$\left[J_a^{\alpha}(t-a)^{\beta}\right](t) = \frac{\Gamma(\beta+1)}{\Gamma(\beta+\alpha+1)}(t-a)^{\beta+\alpha}, \qquad \alpha \geqslant 0, \quad \beta>0. \tag{4}$$

Definition 2.5 *The generalized Mittag-Leffler function (also called two-parameter Mittag-Leffler function) is defined as:*

$$E_{\alpha,\beta}(z) = \sum_{k=0}^{\infty}\frac{z^k}{\Gamma(\alpha k+\beta)}, \quad \beta, z \in \mathbb{C}, \quad Re(\alpha)>0. \tag{5}$$

When $\beta = 1$, a special case of this function is obtained, called a one-parameter Mittag-Leffler function, given as:

$$E_{\alpha}(z) = E_{\alpha,1}(z) = \sum_{k=0}^{\infty}\frac{z^k}{\Gamma(\alpha k+1)}, \quad z \in \mathbb{C}, \quad \mathrm{Re}(\alpha)>0. \tag{6}$$

Taking different values for α and β, we see that this function represents many important special cases, such as:

$$\begin{aligned} E_{1,1}(z) &= e^z, & E_{1,2}(z) &= \frac{e^z-1}{z}, \\ E_{2,1}(z) &= \cosh(\sqrt{z}), & E_{2,2}(z) &= \frac{\sinh(\sqrt{z})}{\sqrt{z}}, \\ E_{2,1}(-z^2) &= \cos(z), & E_{0,1}(z) &= \frac{1}{1-z}, \quad |z|<1. \end{aligned}$$

The generalized Mittag-Leffler function is an entire function [32, 33], so bounded in any finite interval.

Lemma 2.2 *[34] Let $0<\alpha\leq 1$, and $\lambda>0$. Then, the function $E_{\alpha,\beta}(-\lambda z^{\alpha})$, $\alpha \leq \beta$ is positive monotonically decreasing functions of $z>0$.*

Definition 2.6 *Let $n-1<\alpha\leq n$. Then the Laplace transform of the Caputo's fractional derivative is given as*

$$\mathcal{L}\left\{\mathcal{D}^{\alpha}N(t)\right\}(s) = s^{\alpha}\mathcal{N}(s) + \sum_{k=0}^{n-1}s^{n-k-1}N^{(k)}(0_+), \quad Re(s)>0, \tag{7}$$

where $Re(\alpha)>0$.

Preprints (www.preprints.org) | NOT PEER-REVIEWED | Posted: 2 April 2021 doi:10.20944/preprints202104.0052.v1

Lemma 2.3 *Consider the two-parameter Mittag-Leffler function, the Laplace transform formula is given*

$$\mathcal{L}\left\{t^{\beta-1}E_{\alpha,\beta}(\lambda^* t^\alpha)\right\}(s) = \frac{s^{\alpha-\beta}}{s^\alpha - \lambda^*}, \quad Re(z) > 0 \quad |\lambda^* s^{-\alpha}| < 1, \tag{8}$$

where $\alpha, \beta, \lambda^* \in \mathbb{C}$, $Re(\alpha) > 0$, $Re(\beta) > 0$.

Lemma 2.4 *[35] For* $0 < \alpha \leq 1$, *let* $\varphi \in C[a,b]$ *and* $\mathcal{D}^\alpha \in (a,b]$. *Then*

$$u(t) = u(a) + \frac{1}{\Gamma(\alpha)}\mathcal{D}^\alpha u(\eta)(t-a)^\alpha, \qquad 0 \leq \eta \leq t, \forall t \in (a,b]. \tag{9}$$

Lemma 2.4 is called the generalized mean value Theorem.

3 Model formulation

In this section we develop a compartmental COVID-19 model where individuals are classified at time t as: susceptible (S), Exposed (E), Exposed but quarantined (Q_1), Infected (I), infected but quarantined (Q_2), and Recovered (R). The infected compartment, I, contains both asymptomatic and symptomatic carriers who have not been clinically confirmed COVID-19 positive. Transmission of COVID-19 occurs as a result of touching a contaminated surface or sharing very close space (less than 6 ft/ 2m) with an infectious host coughing or sneezing [36]. We assume that exposed and infected individuals are able to transmit the disease to the general public, but quarantined individuals, either exposed or infected, are unable to transmit the virus to general public because they stay in isolation. Susceptible individuals contract the disease at a rate β. Once individuals are confirmed positive, they are placed in self-quarantine (or hospitalize) at rate k_4. Individuals in I and Q_2 decrease by diseased-induced death rate δ. There are several reports that recovered individuals are susceptible to re-infection; WHO on April 24, 2020, reported that there is currently no evidence that people who have recovered from COVID-19 and have antibodies are protected from a second infection [1]. Because of this, we take into consideration loss of immunity at rate ρ_2. See Figure 1 for an illustration of the model and Table 1 for the meaning of the remaining parameters.

Preprints (www.preprints.org) | NOT PEER-REVIEWED | Posted: 2 April 2021 doi:10.20944/preprints202104.0052.v1

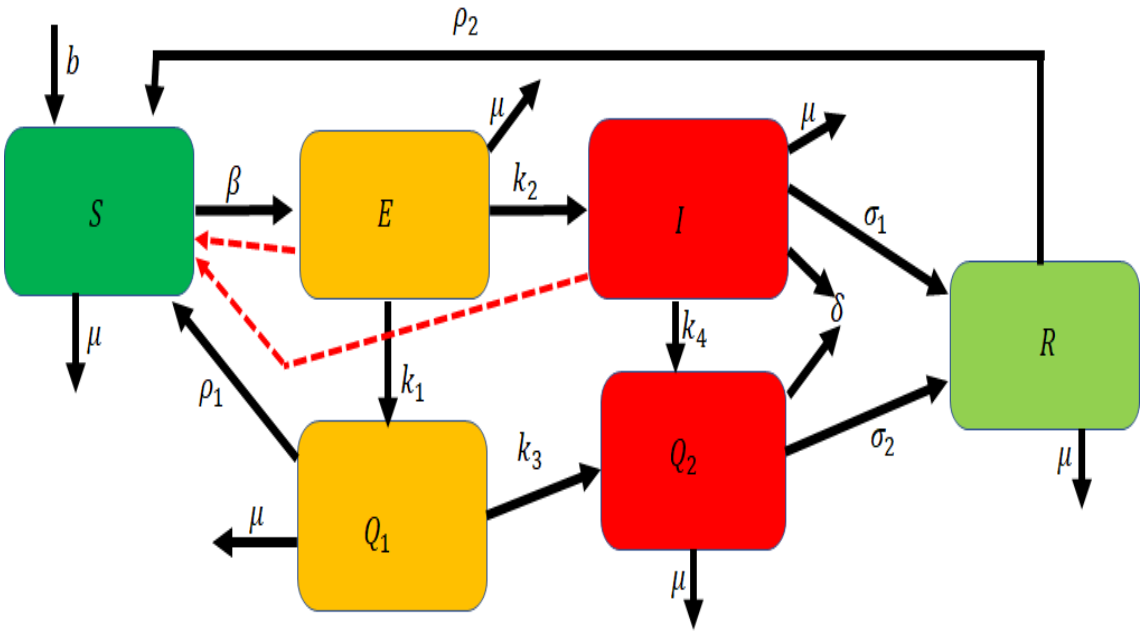

Figure 1: Flow diagram of the COVID-19 model.

A nonlinear system under the above transmission assumptions is given by

$$\begin{aligned}
\frac{d^\alpha S}{dt^\alpha} &= b - \beta(E+I)S + \rho_1 Q_1 + \rho_2 R - \mu S \\
\frac{d^\alpha E}{dt^\alpha} &= \beta(E+I)S - (k_1 + k_2 + \mu)E \\
\frac{d^\alpha Q_1}{dt^\alpha} &= k_1 E - (\rho_1 + k_3 + \mu)Q_1 \\
\frac{d^\alpha I}{dt^\alpha} &= k_2 E - (k_4 + \sigma_1 + \delta + \mu)I \\
\frac{d^\alpha Q_2}{dt^\alpha} &= k_3 Q_1 + k_4 I - (\sigma_2 + \delta + \mu)Q_2 \\
\frac{d^\alpha R}{dt^\alpha} &= \sigma_1 I + \sigma_2 Q_2 - (\rho_2 + \mu)R
\end{aligned} \tag{10}$$

and initial points to be

$$\begin{aligned}
S(0) &= S_0 \\
E(0) &= E_0 \\
Q_1(0) &= Q_{1,0} \\
I(0) &= I_0 \\
Q_2(0) &= Q_{2,0} \\
R(0) &= R_0
\end{aligned} \tag{11}$$

with $0 < \alpha \leq 1$, $\frac{d^\alpha}{dt^\alpha}$ the Caputo fractional derivative of order α, where b, μ are birth and per capital death rates of individuals respectively. All the parameters are defined and

Preprints (www.preprints.org) | NOT PEER-REVIEWED | Posted: 2 April 2021 doi:10.20944/preprints202104.0052.v1

values provided in the Table 1 below. Note that $N = S + E + Q_1 + I + Q_2 + R$. This means that

$$\frac{d^{\alpha}N}{dt^{\alpha}} = b - \delta(I + Q_2) - \mu N$$

.

Table 1: Parameters of the disease model and their meanings.

Parameter	Likely range (Sources)	Default value
b (Recruitment rate of the population)	$\mu \times N(0)$	78680
β (Effective contact rate)	$2.1011 \times 10^{-8} - 9.11 \times 10^{-8}$ [38, 39]	4.1011×10^{-8} day^{-1}
ρ_1(Transition rate from exposed quarantined to susceptible individuals)	1/14 [38]	1/14
ρ_2(Transition rate from recovered to susceptible individuals)	Assumed	5/100
k_1(Quarantine rate of exposed individuals)	1/10[39]	1/10 day^{-1}
k_2 (Transition rate from exposed to infected class $I(t)$)	1/14–1/3 [38, 40, 41]	1/7 day^{-1}
k_3 (Transition from exposed quarantined to infected quarantined)	0.1259 [38]	0.1259
k_4 (Quarantining rate of individuals in the $I(t)$ class)	0.2– 1 [42, 38]	0.3654 day^{-1}
δ(Disease-induced death rate)	1.7826×10^{-5}[38, 39]	1.7826×10^{-5}
μ (Natural death rate)	7.1/1000	7.1/1000
σ_1 (Natural recovery rate)	1/30–1/3 day^{-1} [38, 43]	1/20 day^{-1}
σ_2 (Recovery rate of quarantine infected)	0.11624 [38, 44]	0.11624 day^{-1}
$S(0)$ (Initial value of the susceptible)	[39]	11081000
$E(0)$ (Initial value of the expose)	[39]	399
$Q_1(0)$(Initial value of the expose,quarantined)	[39]	159
$I(0)$ (Initial value of the infected)	[39]	54
$Q_2(0)$ (Initial value of the infected, quarantined)	[39]	28
$R(0)$ (Initial value of the recovered)	[39]	12

4 Analysis of the Time-Fractional COVID-19 Model

Our focus in this Section is on detailed analysis of the proposed COVID-19 model of time-fractional type. The existence, uniqueness, and non-negativity results of solutions to the system 10-11 are presented and proven. We further we investigate conditions and results on existence, stability (local and global) and equilibrium of the proposed model.

Preprints (www.preprints.org) | NOT PEER-REVIEWED | Posted: 2 April 2021 doi:10.20944/preprints202104.0052.v1

Let us define a feasible region Δ of system (10)-11 as:

$$\nabla = \left\{ x = (S, E, Q_1, I, Q_2, R) \in \mathbb{R}^6_+ : S \geq 0, N \leq \frac{b}{\mu} \right\}.$$

The region is an area which contains all biologically and mathematically relevant solutions of system 10-11.
We denote the following parameter for easy calculation.

$$\begin{aligned}
\gamma_1 &= k_1 + k_2 + \mu \\
\gamma_2 &= \rho_1 + k_3 + \mu \\
\gamma_3 &= \sigma_2 + \delta + \mu \\
\gamma_4 &= k_4 + \sigma_1 + \delta + \mu \\
\gamma_5 &= k_2 + k_4 + \sigma_1 + \delta + \mu.
\end{aligned}$$

4.1 Results on the Existence and Uniqueness of Solutions

The following Lemma is needed to prove the existence and uniqueness of solutions to the system considered in 10-11. Our results include forward-invariant property of the domain considered.

Lemma 4.1
For $0 < \alpha \leq 1$, let $u \in C[0, b]$ and $\mathcal{D}^\alpha u \in (0, b]$. Then

(a) the function u is non-decreasing if $\mathcal{D}^\alpha u(t) \geq 0$, $\forall\, t \in (0, b)$.

(b) the function u is non-increasing if $\mathcal{D}^\alpha u(t) \leq 0$, $\forall\, t \in (0, b)$.

Proof. The proof is a direct consequence of Lemma 2.4.

Theorem 4.1
The initial valued problem for the COVID-19 model of fractional order type in 10-11 has unique solution in ∇.

Proof. Using Theorem (3.1) and Remark (3.2) in [45], the existence and uniqueness of solution in $(0, \infty)$ is obtained. Furthermore, we need to show that the closed set ∇ is forward-invariant w.r.t (10). To prove this, we first consider the fractional differential:

$$\frac{d^\alpha N}{dt^\alpha} = b - \mu N.$$

Using the Laplace transform given in 2.6 in both sides, we obtain

$$s^\alpha \mathcal{N}(s) - s^{\alpha-1} N(0) = \frac{b}{s} - \mu \mathcal{N}(s). \tag{12}$$

Re-arranging 12, we get

$$\mathcal{N}(s) = b \frac{1}{s(s^\alpha + \mu)} + N(0) \frac{s^{\alpha-1}}{(s^\alpha + \mu)}. \tag{13}$$

Preprints (www.preprints.org) | NOT PEER-REVIEWED | Posted: 2 April 2021 doi:10.20944/preprints202104.0052.v1

Applying Laplace inverse transform, and Lemma 2.3 after some simplification, we obtain the solution as

$$N(t) = N(0)E_\alpha(-\mu t^\alpha) + \frac{b}{\mu}\left[1 - E_\alpha(-\mu t^\alpha)\right]. \tag{14}$$

Recall that

$$\frac{d^\alpha N}{dt^\alpha} = b - \delta(I + Q_2) - \mu N \leq b - \mu N.$$

Using 14 combined with Lemma 2.2, it follows that

$$\limsup_{t\to\infty} N(t) \leq \frac{b}{\mu}.$$

Thus, ∇ is positive and bounded. So all solutions of the system (10)-11 are confined in the set ∇.

4.2 Existence, Stability and Equilibrium Results for COVID-19 Model of Fractional Type

From above, the region ∇ is positively-invariant under models (10)-(11). Then the system is both epidemiologically and mathematically well-posed. Therefore, it is sufficient to study the dynamics of the model in ∇.

In the absence of COVID-19, we have $E = Q_1 = I = Q_2 = 0$ and at equilibrium

$$S^* = N^* \to \frac{b}{\mu}.$$

There exists a disease-free equilibrium of system (10) given by

$$DFE = \left(\frac{b}{\mu}, 0, 0, 0, 0, 0\right). \tag{15}$$

4.2.1 Computation of $\mathcal{R}_0$

A crucial mathematical quantity of major public health interest is the basic reproduction number of the model (denoted by $\mathcal{R}_0$). In [46], the basic Reproductive Number is defined as the average number of secondary infections that occur when one infected individual is introduced into a completely susceptible population. It is one of the most significant thresholds when studying infectious disease models and it quantifies the intensity of an outbreak of diseases. It also plays important role in evaluating control strategies. We will use the next generation approach described in [47, 48, 49] to compute $\mathcal{R}_0$ of our model. This method is defined as the dominant eigenvalue (spectral radius) of the matrix FV^{-1}, where F and V^{-1} are matrices determined as:

$$F_i = \begin{bmatrix} F_E \\ F_{Q_1} \\ F_I \\ F_{Q_2} \end{bmatrix} = \begin{bmatrix} \beta(E+I)S \\ 0 \\ 0 \\ 0 \end{bmatrix}$$

Preprints (www.preprints.org) | NOT PEER-REVIEWED | Posted: 2 April 2021 doi:10.20944/preprints202104.0052.v1

and

$$V_i = \begin{bmatrix} V_E \\ V_{Q_1} \\ V_I \\ V_{Q_2} \end{bmatrix} = \begin{bmatrix} \gamma_1 E \\ -k_1 E + \gamma_2 Q_1 \\ -k_2 E + \gamma_4 I \\ -k_3 Q_1 - k_4 I + \gamma_3 Q_2 \end{bmatrix}.$$

Therefore

$$F = \begin{bmatrix} \beta S^* & 0 & \beta S^* & 0 \\ 0 & 0 & 0 & 0 \\ 0 & 0 & 0 & 0 \\ 0 & 0 & 0 & 0 \end{bmatrix}.$$

and

$$V = \begin{bmatrix} \gamma_1 & 0 & 0 & 0 \\ -k_1 & \gamma_2 & 0 & 0 \\ -k_2 & 0 & \gamma_4 & 0 \\ 0 & -k_3 & -k_4 & \gamma_3 \end{bmatrix},$$

where $S^* = \frac{b}{\mu}$.

The basic reproduction number ($\mathcal{R}_0$) is the spectral radius of $|FV^{-1} - \lambda I|$ and is given by

$$\mathcal{R}_0 = \frac{b\beta\gamma_5}{\mu\gamma_1\gamma_4} \tag{16}$$

4.2.2 Stability Results

Theorem 4.1 (Local Stability)
The disease-free equilibrium $\left(\frac{b}{\mu}, 0, 0, 0, 0, 0\right)$ *of system 10 is locally asymptotically stable if* $\mathcal{R}_0 < 1$ *and unstable if* $\mathcal{R}_0 > 1$.

Proof. To determine the local stability of the disease-free equilibrium, we use the eigenvalues of the associated Jacobian matrix. The Jacobian matrix of system (3) at

$$DFE = \left(\frac{b}{\mu}, 0, 0, 0, 0, 0\right)$$

is

$$J = \begin{pmatrix} -\mu & -\frac{b\beta}{\mu} & \rho_1 & -\frac{b\beta}{\mu} & 0 & \rho_2 \\ 0 & \frac{b\beta}{\mu} - \gamma_1 & 0 & \frac{b\beta}{\mu} & 0 & 0 \\ 0 & k_1 & -\gamma_2 & 0 & 0 & 0 \\ 0 & k_2 & 0 & -\gamma_4 & 0 & 0 \\ 0 & 0 & k_3 & k_4 & -\gamma_3 & 0 \\ 0 & 0 & 0 & \sigma_1 & \sigma_2 & -(\rho_2 + \mu) \end{pmatrix}.$$

The characteristic equation of the Jacobian matrix is

$$(\lambda + \mu)(\lambda + \rho_2 + \mu)(\lambda + \gamma_2)(\lambda + \gamma_3)\left(\lambda^2 + a_1\lambda + a_0\right) = 0,$$

where

$$a_1 = -\gamma_1(\mathcal{R}_0 - 1) + \gamma_4 + \frac{b\beta k_2}{\mu\gamma_4}$$
$$a_0 = -\gamma_1\gamma_4(\mathcal{R}_0 - 1).$$

Preprints (www.preprints.org) | NOT PEER-REVIEWED | Posted: 2 April 2021 doi:10.20944/preprints202104.0052.v1

For $\mathcal{R}_0 < 1$, all the roots of the characteristic equation have negative real parts.
The public health implication of Theorem 4.1 is that COVID-19 can be eliminated or controlled when $\mathcal{R}_0 < 1$, if the initial sizes of the subpopulations of the model are in the basin of attraction of the DFE (∇). Global stability of the DFE is necessary to ensure that the disease elimination is independent of the initial sizes of the subpopulations[50].

Theorem 4.2 (Global Stability)
The disease-free equilibrium $\left(\frac{b}{\mu}, 0, 0, 0, 0, 0\right)$ *of system 10 is globally asymptotically stable if* $\mathcal{R}_0 < 1$.

Proof. Consider the Lyapunov function $V = (S, E, Q_1, I, Q_2, R) : \mathbb{R}^6_+$ defined as

$$V = E + \frac{\beta b}{\mu\gamma_4} I.$$

Then

$$\begin{aligned}
\frac{d^\alpha V}{dt^\alpha} =& \frac{d^\alpha E}{dt^\alpha} + \frac{\beta b}{\mu\gamma_4}\frac{d^\alpha I}{dt^\alpha} \\
=& \beta(E+I)S - \gamma_1 E + \frac{\beta b}{\mu\gamma_4}\left[k_2 E - \gamma_4 I\right] \\
=& \beta ES - \gamma_1 E + \frac{\beta b}{\mu\gamma_4} k_2 E + \beta IS - \frac{\beta b}{\mu} I \\
\leq& \beta ES^* - \gamma_1 E + \frac{\beta b}{\mu\gamma_4} k_2 E + \beta IS^* - \frac{\beta b}{\mu} I \\
=& \left(\frac{\beta b}{\mu} - \gamma_1\right) E + \frac{\beta b k_2 E}{\mu\gamma_4} \\
=& \gamma_1\left(\frac{\beta b\gamma_4}{\mu\gamma_1\gamma_4} - 1\right) E + \frac{\beta b k_2 E}{\mu\gamma_4} \\
=& \gamma_1\left(\frac{\beta b\gamma_5}{\mu\gamma_1\gamma_4} - 1\right) E - \frac{\beta b k_2 E}{\mu\gamma_4} + \frac{\beta b k_2 E}{\mu\gamma_4} \\
=& \gamma_1\left(\mathcal{R}_0 - 1\right) E.
\end{aligned}$$

We have $\frac{d^\alpha V}{dt^\alpha} = 0$ when $E = 0$, and $\frac{d^\alpha V}{dt^\alpha} < 0$ when $E > 0$ provided that $\mathcal{R}_0 < 1$. It follows from the the generalized Lasalle invariance principle [51] that the disease-free equilibrium is globally asymptotically stable.

4.2.3 Computation of an Endemic Equilibrium

Next, we summarize the predictions of endemic equilibrium of model 10 in the following lemma.

Lemma 4.3 (Equilibrium)
Let

$$A_1 = \frac{(\rho_1(k_2+\mu) + \gamma_1\gamma_4(k_3+\mu))}{k_2\gamma_2} > 0$$
$$A_2 = \sigma_1 + \frac{\sigma_2 k_3 k_1 \gamma_4}{k_2\gamma_2\gamma_3} + \frac{\sigma_2 k_4}{\gamma_3} > 0.$$

Preprints (www.preprints.org) | NOT PEER-REVIEWED | Posted: 2 April 2021 doi:10.20944/preprints202104.0052.v1

(a). If $\mathcal{R}_0 > 1$ *and*

(i) $\rho_2 = 0$, *then the model* (10) *has a unique endemic equilibrium.*

(ii) $\dfrac{\rho_2}{\rho_2+\mu} < \dfrac{A_1}{A_2}$, *then the model* (10) *has a unique endemic equilibrium.*

(b). If $\mathcal{R}_0 < 1$ *and* $\dfrac{\rho_2}{\rho_2+\mu} > \dfrac{A_1}{A_2}$, *then the model* (10) *has a unique endemic equilibrium.*

Proof. The endemic equilibrium is the solution of

$$\begin{aligned} b-\beta(E^{**}+I^{**})S^{**}+\rho_1 Q_1^{**}+\rho_2 R^{**}-\mu S &= 0\\ \beta(E^{**}+I^{**})S^{**}-\gamma_1 E^{**} &= 0\\ k_1 E^{**}-\gamma_2 Q_1^{**} &= 0\\ k_2 E^{**}-\gamma_4 I^{**} &= 0\\ k_3 Q_1^{**}+k_4 I^{**}-\gamma_3 Q_2^{**} &= 0\\ \sigma_1 I^{**}+\sigma_2 Q_2^{**}-(\rho_2+\mu)R^{**} &= 0. \end{aligned} \tag{17}$$

It follows that

$$\begin{aligned} E^{**} &= \frac{\gamma_4}{k_2} I^{**}\\ Q_1^{**} &= \frac{k_1}{\gamma_2} E^{**} = \frac{k_1\gamma_4}{k_2\gamma_2} I^{**}\\ Q_2^{**} &= \frac{k_3 Q_1^{**}+k_4 I^{**}}{\gamma_3} = \frac{k_3k_1\gamma_4+k_4k_2\gamma_2}{k_2\gamma_2\gamma_3} I^{**}\\ R^{**} &= \frac{\sigma_1 I^{**}+\sigma_2 Q_2^{**}}{(\rho_2+\mu)} = \frac{\sigma_1 k_2\gamma_2\gamma_3+\sigma_2\left(k_3k_1\gamma_4+k_4k_2\gamma_2\right)}{k_2\gamma_2\gamma_3(\rho_2+\mu)} I^{**}\\ S^{**} &= \frac{\gamma_1 E^{**}}{\beta(E^{**}+I^{**})} \end{aligned} \tag{18}$$

Substitute the last line of equation (18) into the first line of equation (17) to obtain

$$\begin{aligned} & b-\beta(E^{**}+I^{**})\frac{\gamma_1 E^{**}}{\beta(E^{**}+I^{**})}+\rho_1 Q_1^{**}+\rho_2 R^{**}-\frac{\mu\gamma_1 E^{**}}{\beta(E^{**}+I^{**})} = 0\\ & b-\gamma_1 E^{**}+\rho_1 Q_1^{**}+\rho_2 R^{**}-\frac{\mu\gamma_1 E^{**}}{\beta(E^{**}+I^{**})} = 0\\ & b\beta(E^{**}+I^{**})-\gamma_1 E^{**}\beta(E^{**}+I^{**})+\rho_1 Q_1^{**}\beta(E^{**}+I^{**})+\rho_2 R^{**}\beta(E^{**}+I^{**})\\ & -\mu\gamma_1 E^{**} = 0 \end{aligned} \tag{19}$$

Let

$$\begin{aligned} B_1 &= \frac{\gamma_4}{k_2}\\ B_2 &= \frac{k_1\gamma_4}{k_2\gamma_2} = \frac{k_1 B_1}{\gamma_2}\\ B_3 &= \frac{\sigma_1 k_2\gamma_2\gamma_3+\sigma_2\left(k_3k_1\gamma_4+k_4k_2\gamma_2\right)}{k_2\gamma_2\gamma_3(\rho_2+\mu)}\\ &= \frac{1}{\rho_2+\mu}\left(\sigma_1+\frac{\sigma_2 k_3k_1B_1}{\gamma_2\gamma_3}+\frac{\sigma_2 k_4}{\gamma_3}\right). \end{aligned} \tag{20}$$

Preprints (www.preprints.org) | NOT PEER-REVIEWED | Posted: 2 April 2021 doi:10.20944/preprints202104.0052.v1

Then

$$b\beta(B_1I^{**}+I^{**})-\gamma_1B_1I^{**}\beta(B_1I^{**}+I^{**})+\rho_1B_2I^{**}\beta(B_1I^{**}+I^{**})+\rho_2B_3I^{**}\beta(B_1I^{**}+I^{**}) - \mu\gamma_1B_1I^{**}=0 \tag{21}$$

$$\left[b\beta(B_1+1)-\gamma_1B_1\beta(B_1+1)I^{**}+\rho_1B_2\beta(B_1+1)I^{**}+\rho_2B_3\beta(B_1+1)I^{**}-\mu\gamma_1B_1\right]I^{**}=0 \tag{22}$$

For $I^{**}\neq 0$, we get

$$b\beta(B_1+1)-\mu\gamma_1B_1-\left[\gamma_1B_1\beta(B_1+1)-\rho_1B_2\beta(B_1+1)-\rho_2B_3\beta(B_1+1)\right]I^{**}=0,$$

which leads to

$$\begin{aligned}
I^{**} &= \frac{b\beta(B_1+1)-\mu\gamma_1B_1}{\gamma_1B_1\beta(B_1+1)-\rho_1B_2\beta(B_1+1)-\rho_2B_3\beta(B_1+1)} \\
&= \frac{b\beta+B_1\left(b\beta-\mu\gamma_1\right)}{\beta(B_1+1)\left[\gamma_1B_1-\rho_1B_2-\rho_2B_3\right]} \\
&= \frac{\mu\gamma_1B_1\left(\mathcal{R}_0-1\right)}{\beta(B_1+1)\left[\gamma_1B_1-\rho_1B_2-\rho_2B_3\right]} \\
&= \frac{\mu\gamma_1B_1\left(\mathcal{R}_0-1\right)}{\beta(B_1+1)\left[\gamma_1B_1-\frac{\rho_1k_1B_1}{\gamma_2}-\frac{\rho_2}{\rho_2+\mu}\left(\sigma_1+\frac{\sigma_2k_3k_1B_1}{\gamma_2\gamma_3}+\frac{\sigma_2k_4}{\gamma_3}\right)\right]} \\
&= \frac{\mu\gamma_1B_1\left(\mathcal{R}_0-1\right)}{\beta(B_1+1)\left[\frac{\rho_1(k_2+\mu)+(k_3+\mu)\gamma_1}{\gamma_2}B_1-\frac{\rho_2}{\rho_2+\mu}\left(\sigma_1+\frac{\sigma_2k_3k_1B_1}{\gamma_2\gamma_3}+\frac{\sigma_2k_4}{\gamma_3}\right)\right]}.
\end{aligned}$$

Further let

$$\begin{aligned}
A_1 &= \frac{\rho_1(k_2+\mu)+\gamma_1(k_3+\mu)}{\gamma_2}B_1=\frac{\left(\rho_1(k_2+\mu)+\gamma_1(k_3+\mu)\right)\gamma_4}{k_2\gamma_2} \\
A_2 &= \sigma_1+\frac{\sigma_2k_3k_1B_1}{\gamma_2\gamma_3}+\frac{\sigma_2k_4}{\gamma_3}=\sigma_1+\frac{\sigma_2k_3k_1\gamma_4}{k_2\gamma_2\gamma_3}+\frac{\sigma_2k_4}{\gamma_3}.
\end{aligned}$$

Then

$$I^{**}=\frac{\mu\gamma_1B_1\left(\mathcal{R}_0-1\right)}{A_2\beta(B_1+1)\left(\frac{A_1}{A_2}-\frac{\rho_2}{\rho_2+\mu}\right)}. \tag{23}$$

It follows from (23) that $I^{**}>0$ if

1. $\mathcal{R}_0>1$ and $\rho_2=0$.
2. $\mathcal{R}_0>1$ and $\dfrac{\rho_2}{\rho_2+\mu}<\dfrac{A_1}{A_2}$.
3. $\mathcal{R}_0<1$ and $\dfrac{\rho_2}{\rho_2+\mu}>\dfrac{A_1}{A_2}$.

Preprints (www.preprints.org) | NOT PEER-REVIEWED | Posted: 2 April 2021 doi:10.20944/preprints202104.0052.v1

4.2.4 Sensitivity Analysis

We carried out sensitivity analysis to identify model parameters that have most influence on the threshold $\mathcal{R}_0$ and the COVID-19 transmission. The index measures the relative change in $\mathcal{R}_0$ with respect to the relative change in the parameters [52, 53, 54]. Sensitivity analysis is useful and can help to identify parameters that need to be targeted in designing control strategies. The parameters b, β have positive impact on the $\mathcal{R}_0$, meaning that, an increase in these parameters implies an increase in $\mathcal{R}_0$. While the $k_1, k_4, \sigma_1, \theta, \mu$ have negative impact on (decrease) the $\mathcal{R}_0$.

Definition 4.1 *The normalized forward sensitivity index of a variable, L, that depends differentially on a parameter, y, is defined as:*

$$\xi_y = \frac{y}{L}\frac{\partial L}{\partial y}.$$

The sensitivity indices of $\mathcal{R}_0$ in terms of the model parameters are as follows.

$$\begin{aligned}
\xi_b &= \frac{b}{\mathcal{R}_0}\frac{\partial \mathcal{R}_0}{\partial b} = 1 \\
\xi_\beta &= \frac{\beta}{\mathcal{R}_0}\frac{\partial \mathcal{R}_0}{\partial \beta} = 1 \\
\xi_{k_1} &= \frac{k_1}{\mathcal{R}_0}\frac{\partial \mathcal{R}_0}{\partial k_1} = -\frac{k_1}{\gamma_1} \\
\xi_{k_2} &= \frac{k_2}{\mathcal{R}_0}\frac{\partial \mathcal{R}_0}{\partial k_2} = \frac{k_2\left(k_1 - k_4 - \sigma_1 - \delta\right)}{\gamma_5\gamma_1} \\
\xi_{k_4} &= \frac{k_4}{\mathcal{R}_0}\frac{\partial \mathcal{R}_0}{\partial k_4} = -\frac{k_2 k_4}{\gamma_4\gamma_5} \\
\xi_{\sigma_1} &= \frac{\sigma_1}{\mathcal{R}_0}\frac{\partial \mathcal{R}_0}{\partial \sigma_1} = -\frac{k_2\sigma_1}{\gamma_4\gamma_5} \\
\xi_\delta &= \frac{\delta}{\mathcal{R}_0}\frac{\partial \mathcal{R}_0}{\partial \delta} = -\frac{k_2\delta}{\gamma_4\gamma_5} \\
\xi_\mu &= \frac{\mu}{\mathcal{R}_0}\frac{\partial \mathcal{R}_0}{\partial \mu} = -\frac{k_2\left(\mu\gamma_1 + \left(\gamma_1 + \mu\right)\gamma_4\right) + \gamma_4^2\left(\gamma_1 + k_4 + \mu\right)}{\gamma_1\gamma_4\gamma_5}.
\end{aligned} \tag{24}$$

It is important to note that a sensitive index can be a constant or depend on other parameters of the model. An $\xi_y = \pm 1$ implies that increasing or decreasing y by a given percentage increases (decreases) always $\mathcal{R}_0$ by that same percentage [55].

Table 2: Sensitivity indices of $\mathcal{R}_0$ based on the parameter values given in Table 1 and equation (24)

Parameter	Sensitivity index
b	1
β	1
k_1	-0.4001
k_2	-0.3188
k_4	-0.2185
δ	-1.0660e-05
μ	-1.3878
σ_1	-0.0299

Preprints (www.preprints.org) | NOT PEER-REVIEWED | Posted: 2 April 2021 doi:10.20944/preprints202104.0052.v1

Based on equation (24) and the sensitivity indices in Table 2, the most of influential parameters are μ, b, β, k_1, k_2. We make the following recommendations.

- Quarantining infected individuals could be an effective control measure against the growing of COVID-19 infection.
- Reducing the transmission parameter is essential in reducing the transmission of the infection. Compliance to protocols such as social distancing, wearing face mask, washing of hands is required to reduce the transmission parameter.

5 Numerical Analysis and Simulation

For completeness, we present in this Section the basic idea behind the method of solution employ to obtain solutions to the proposed system of time fractional model for COVID-19 given in 10.

5.1 Adams-Bashforth-Moulton Method for Fractional Order

Adams-Bashforth-Moulton Method has been applied to integer order differential equations for many years. Here, we give brief description of this method applied to fractional order differential equations. We refer the readers to see [56, 57, 58] for detailed results on stability and convergence. Given the initial valued fractional differential system of the form

$$\frac{d^\alpha}{dt^\alpha}u(t) = \varphi(t, u(t)) \tag{25}$$

and the initial condition

$$u^{(j)}(0) = u_0^j, \qquad j = 0, 1, 2, \cdots, m-1 \tag{26}$$

with $\alpha > 0$, $m = \lceil \alpha \rceil$ and u_0^j, $j = 0, 1, 2, \cdots, m-1$ are given constants which are real numbers. Define the Volterra integral equation as

$$u(t) = \sum_{j=0}^{\lceil \alpha \rceil - 1} \frac{t^j}{j!}u_0^j + \frac{1}{\Gamma(\alpha)}\int_0^t (t-\tau)^{\alpha-1}\varphi(\tau, u(\tau))d\tau \tag{27}$$

Any continuous solution to the initial value fractional differential system 26 is also a solution of the Volterra integral equation given in 27 and vice versa. With the assumption of uniform grid with $t_n = nh$, $n = 0, 1, 2, \cdots, N$, $N \in \mathbb{N}$, $h > 0$ is the step size, we give Adams-Bashforth-Moulton method of fractional order type. We further assume that we first computed the approximation $u_h(t_i) \approx u(t_k)$, $k = 1, 2, \cdots, n$ then find the approximation $u_h(t_{n+1})$ using 27. The derivation for the case $\alpha = 1$ of the one-step Adams-Bashforth-Moulton scheme is similar to the approach used here with some modification making use of the Volterra integral equation in 27. This is a Predictor-Corrector method. The main idea for the corrector is to approximate the integral term in 27 with product Trapezoidal quadrature formula with nodes t_k, $k = 0, 1, 2, \cdots, n+1$. To get the

Preprints (www.preprints.org) | NOT PEER-REVIEWED | Posted: 2 April 2021 doi:10.20944/preprints202104.0052.v1

predictor for this case, product rectangle rule is employed. Define

$$\gamma_{k,n+1} = \begin{cases} n^{\alpha+1} - (n-\alpha)(n+1)^{\alpha} & \text{if } k = 0, \\ 1 & \text{if } k = n+1, \\ (n+2-k)^{\alpha+1} + (n-k)^{\alpha+1} - 2(n+1-k)^{\alpha+1} & \text{if } 1 \leq k \leq n. \end{cases} \tag{28}$$

and

$$\varepsilon_{k,n+1} = \frac{h^{\alpha}}{\alpha}\left[(n+1-k)^{\alpha} - (n-k)^{\alpha}\right]. \tag{29}$$

Then the Adams-Bashforth-Moulton Method for fractional order type which solves system 26 is given ad follows:

$$\begin{aligned} u_h(t_{n+1}) &= \sum_{j=0}^{\lceil\alpha\rceil-1} \frac{t_{n+1}^{j}}{k!} u_0^{j} \\ &\quad + \frac{h^{\alpha}}{\Gamma(\alpha+2)} \varphi\left(t_{n+1}, u_h^{p}(t_{n+1})\right) + \frac{h^{\alpha}}{\Gamma(\alpha+2)} \sum_{k=0}^{n} \gamma_{k,n+1} \varphi\left(t_k, u_h(t_k)\right) \end{aligned} \tag{30}$$

$$u_h^{p}(t_{n+1}) = \sum_{j=0}^{\lceil\alpha\rceil-1} \frac{t_{n+1}^{j}}{j!} u_0^{j} + \frac{1}{\Gamma(\alpha)} \sum_{k=0}^{n} \varepsilon_{k,n+1} \varphi\left(t_k, u_h(t_k)\right), \tag{31}$$

R. Roberto in [59] developed MATLAB subroutine for the implementation of the above method in MATLAB code fde12. With slight modification, we have employed the MATLAB function fde12 for numerical simulation of our proposed time-fractional COVID-19 model given in 26.

5.2 Numerical Simulation and Analysis

Our numerical simulations of the proposed COVID-19 model of time-fractional type are presented here with various analysis. The values of parameters used are as given in Table 1 unless otherwise stated. Effects of the fractional order in the dynamics of the solution profiles obtained for various variables are investigated with meaningful observations. This is an important aspect of our study since the study of the nature and dynamics of COVID-19 (spread, resurgence etc.) is still ongoing and not much is yet to be known. These intrinsic properties of COVID-19 could be captured using fractional derivative in time compared with integer order. Furthermore, we simulate with different values of fractional order with different values of key parameters. The effects of these key parameters are expedient as well to be able to tell what measure is effective in handling the spread of the disease and for crucial decisions given different values of fractional orders as well.

Preprints (www.preprints.org) | NOT PEER-REVIEWED | Posted: 2 April 2021 doi:10.20944/preprints202104.0052.v1

5.2.1 Impact of time-fractional order on the solution profiles for the COVID-19 model

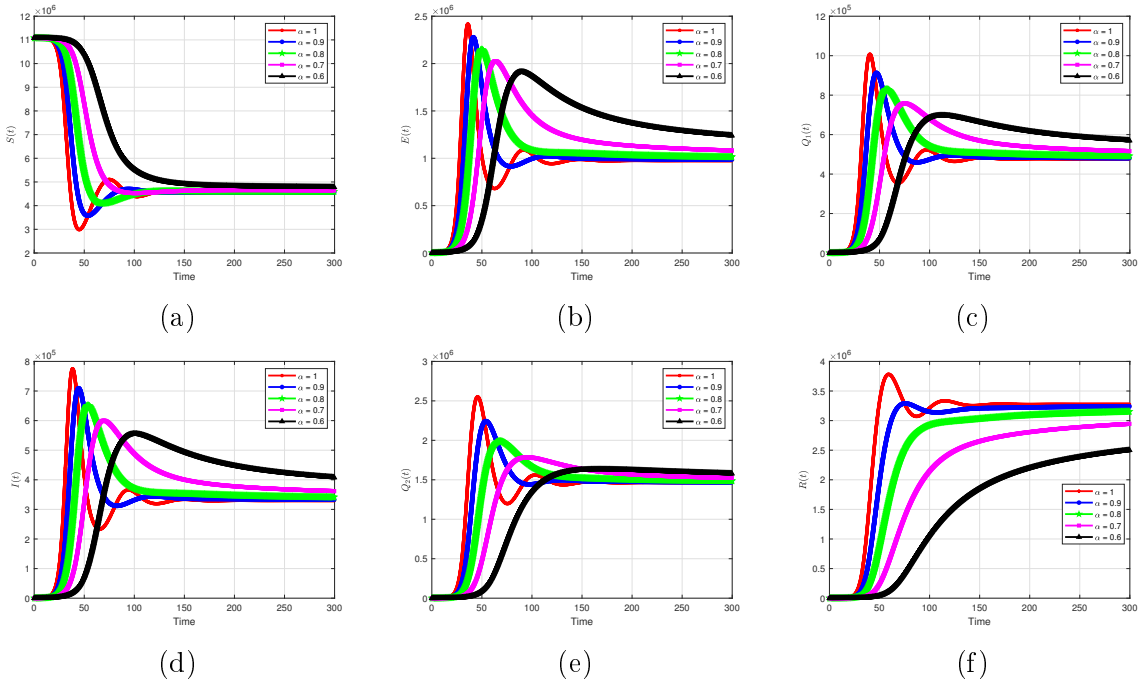

Figure 2: Different α

The proposed COVID-19 model is simulated for different fractional order values $0 < \alpha \leq 1$, using the baseline values of the parameters provided in Table 1. As shown in Figures 2 (a) - (f), the intrinsic properties of the fractional orders are unique; the solution curves display delays in the epidemic peak for different fractional order and flatten faster. For smaller α values, the impact is more pronounced. From a public health perspective, this observation is vital as hospitalization would not be overloaded due to the flattening of the curve. Although the number of infected individuals decreases dramatically for smaller fractional orders, the number of susceptible individuals increases, compare Figure 2 (a) and (d) for $\alpha = 0.6$.

Preprints (www.preprints.org) | NOT PEER-REVIEWED | Posted: 2 April 2021 doi:10.20944/preprints202104.0052.v1

5.2.2 Impact of the effective contact rate on the solution profiles for the COIVD-19 model

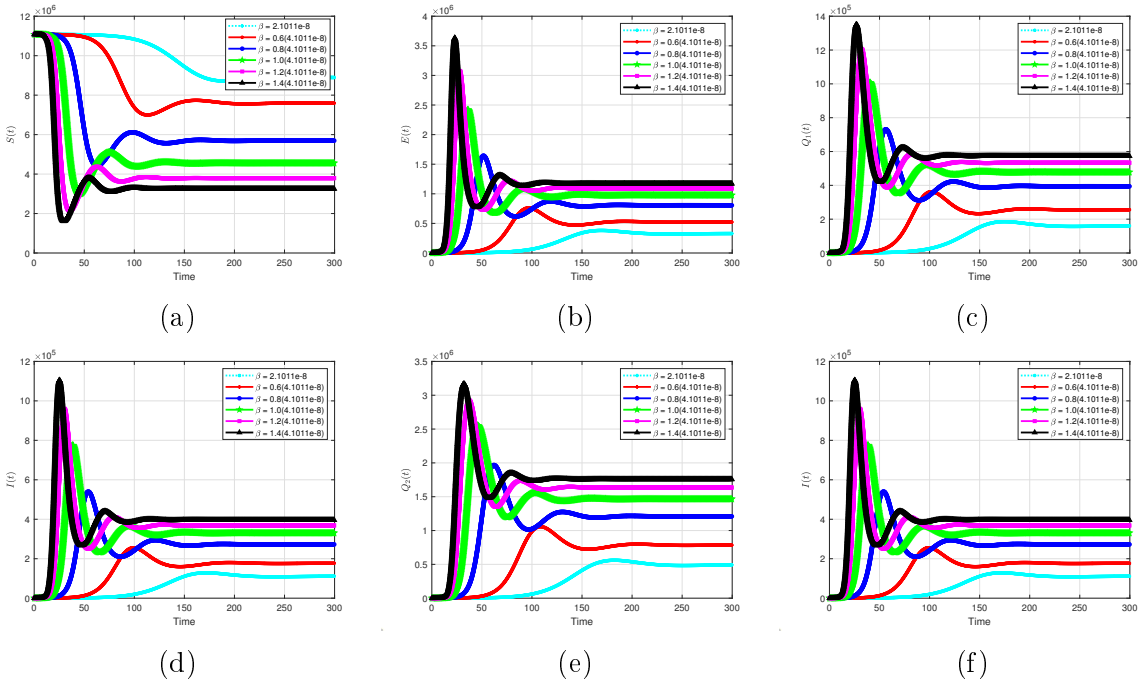

Figure 3: $\alpha = 1$ with different β

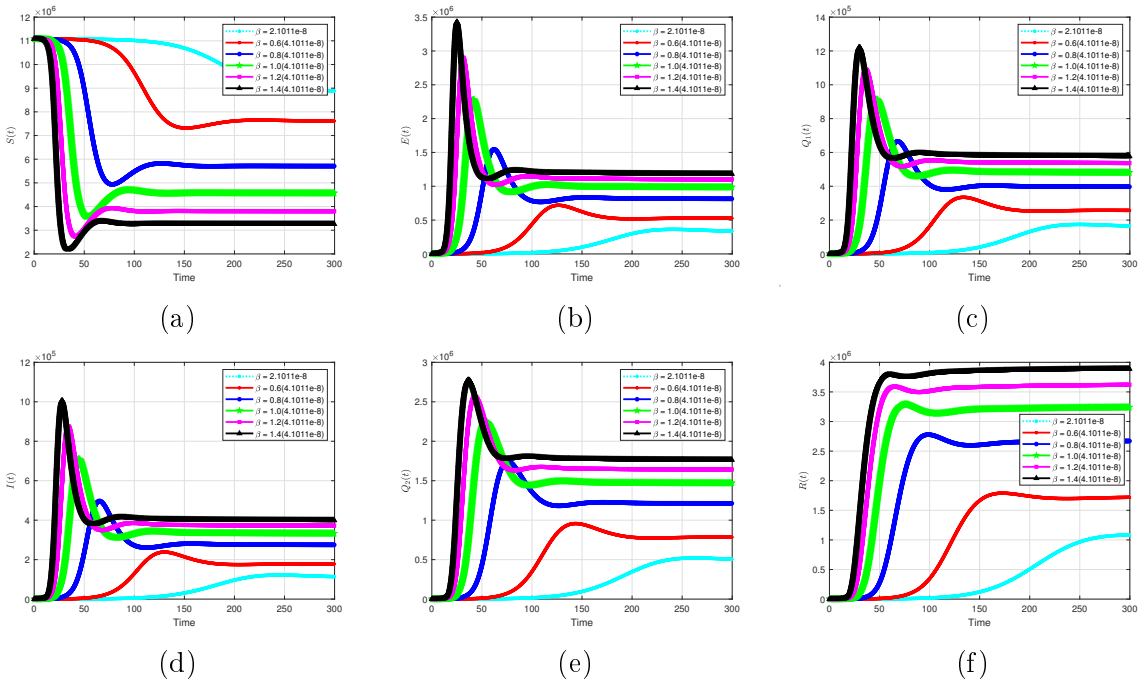

Figure 4: $\alpha = 0.9$ with different β

Preprints (www.preprints.org) | NOT PEER-REVIEWED | Posted: 2 April 2021 doi:10.20944/preprints202104.0052.v1

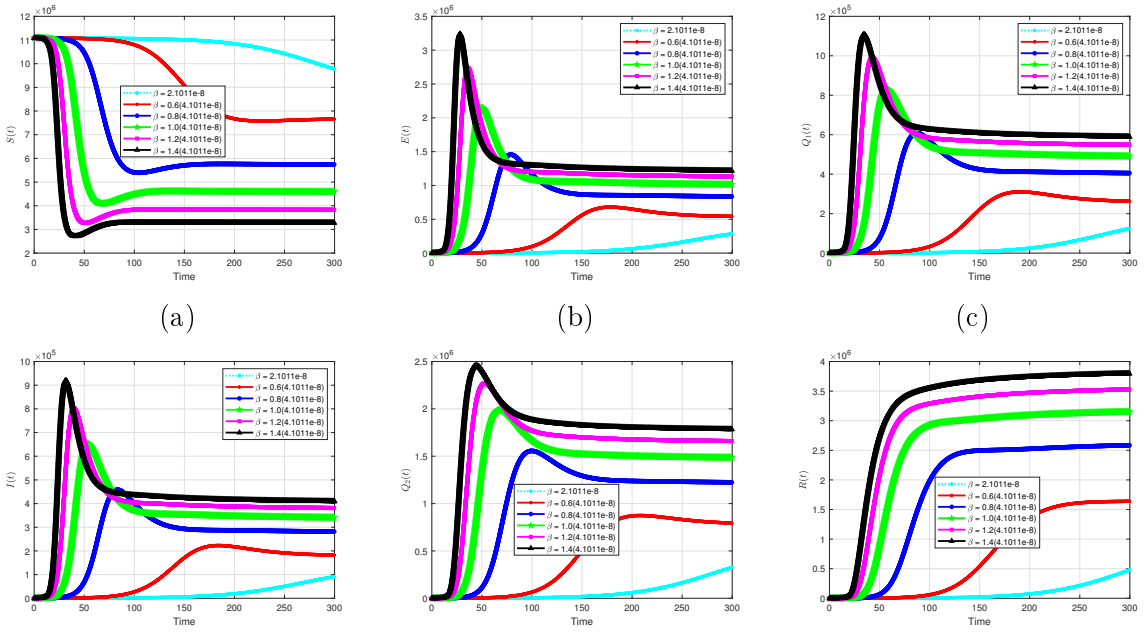

Figure 5: $\alpha = 0.8$ with different β

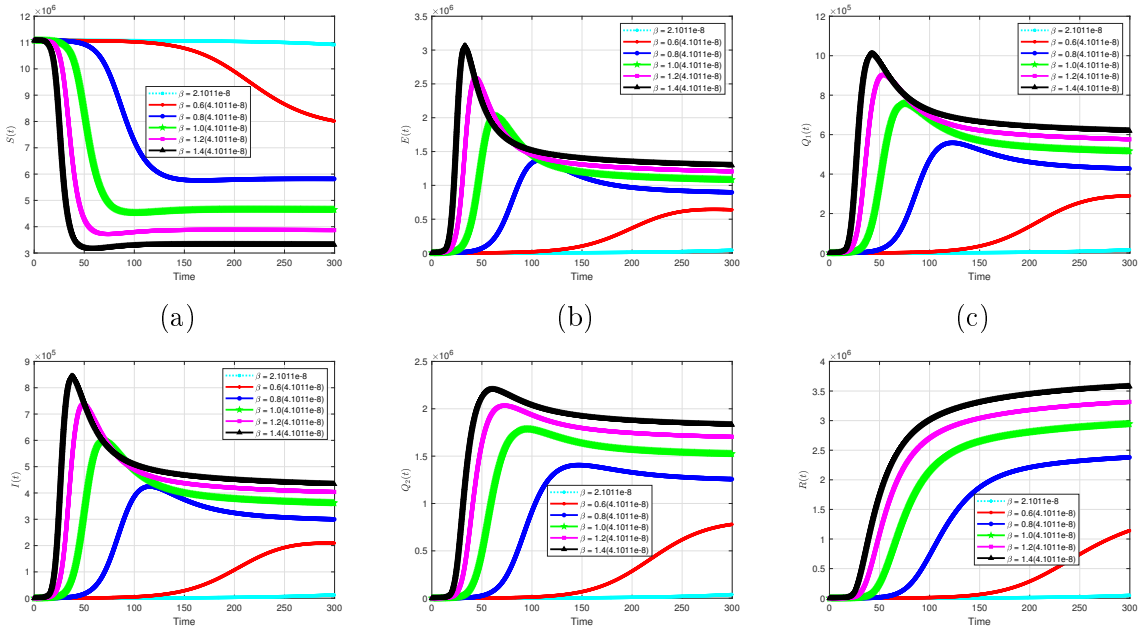

Figure 6: $\alpha = 0.7$ with different β

We investigated the contributions of the effective contact rate on the propagation of the COVID-19. We set the fractional-order as $\alpha = 1, 0.9, 0.8.0.7$, and varied the β. The dynamics of our proposed model for the different values of the transmission parameter are displayed in Figures 3 (a) – (f), 4 (a) – (f), 5 (a) – (f), and 6 (a) – (f), respectively. As the transmission parameter rises, the infected individuals attain a higher peak level,

Preprints (www.preprints.org) | NOT PEER-REVIEWED | Posted: 2 April 2021 doi:10.20944/preprints202104.0052.v1

Figures 3(d), (e), 4 (d), (e), 5 (d), (e), and 6 (d), (e). These effects are consistent with the sensitivity analysis result that shows the influence of the effective contact rate.

5.2.3 Impact of quarantining exposed individuals on the solution profiles for the COIVD-19 model

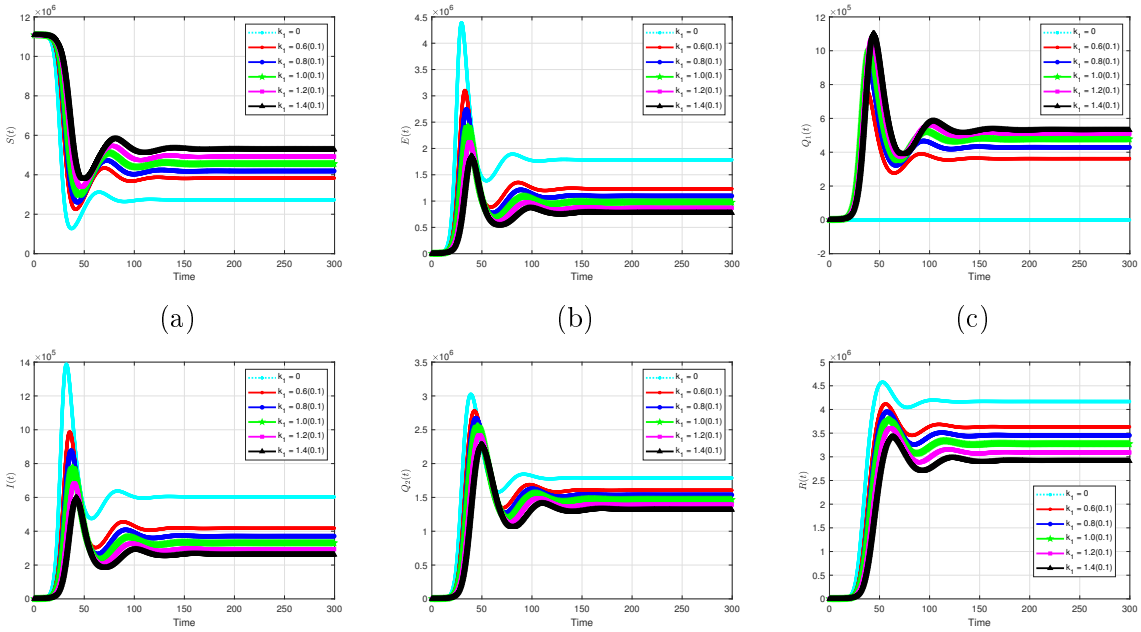

(a) (b) (c)

(d) (e) (f)

Figure 7: $\alpha = 1$ with different k_1

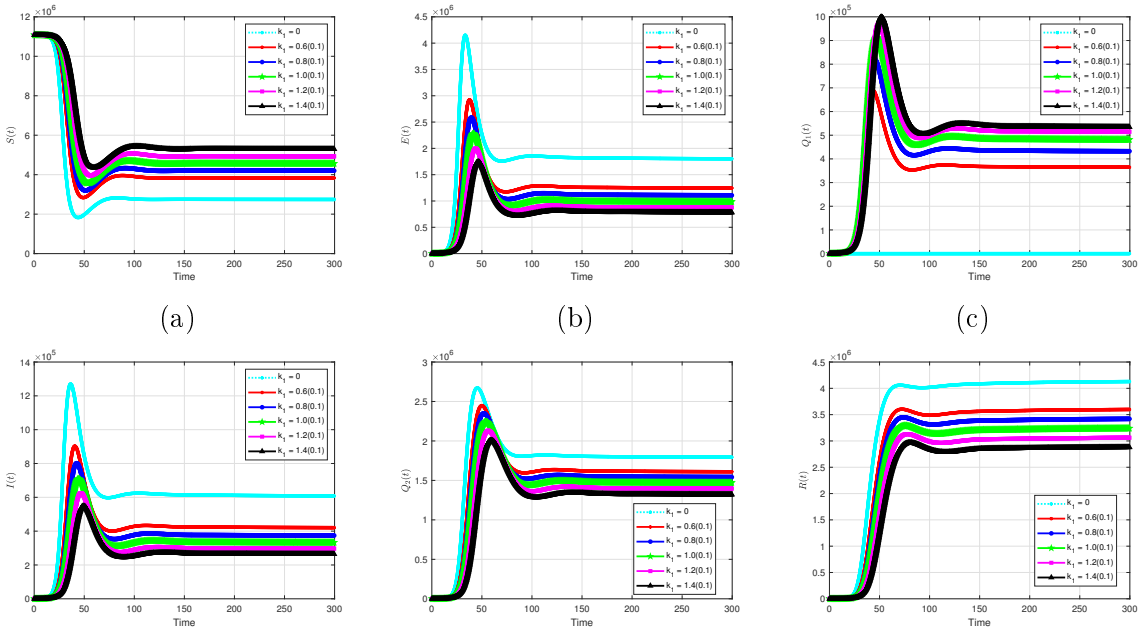

(a) (b) (c)

(d) (e) (f)

Figure 8: $\alpha = 0.9$ with different k_1

Preprints (www.preprints.org) | NOT PEER-REVIEWED | Posted: 2 April 2021 doi:10.20944/preprints202104.0052.v1

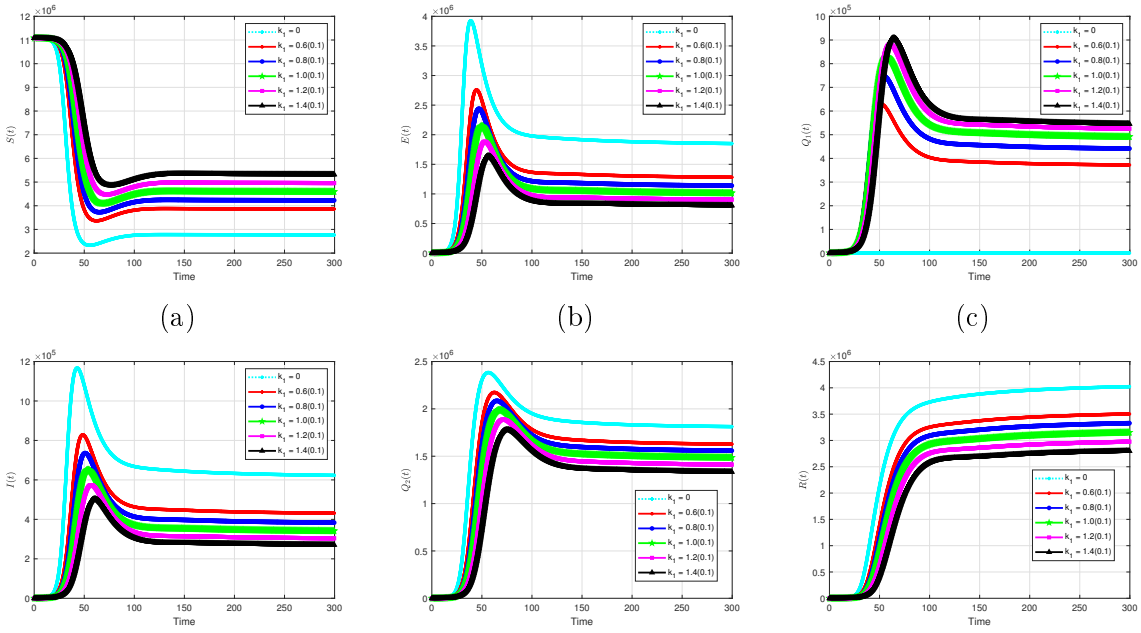

Figure 9: $\alpha = 0.8$ with different k_1

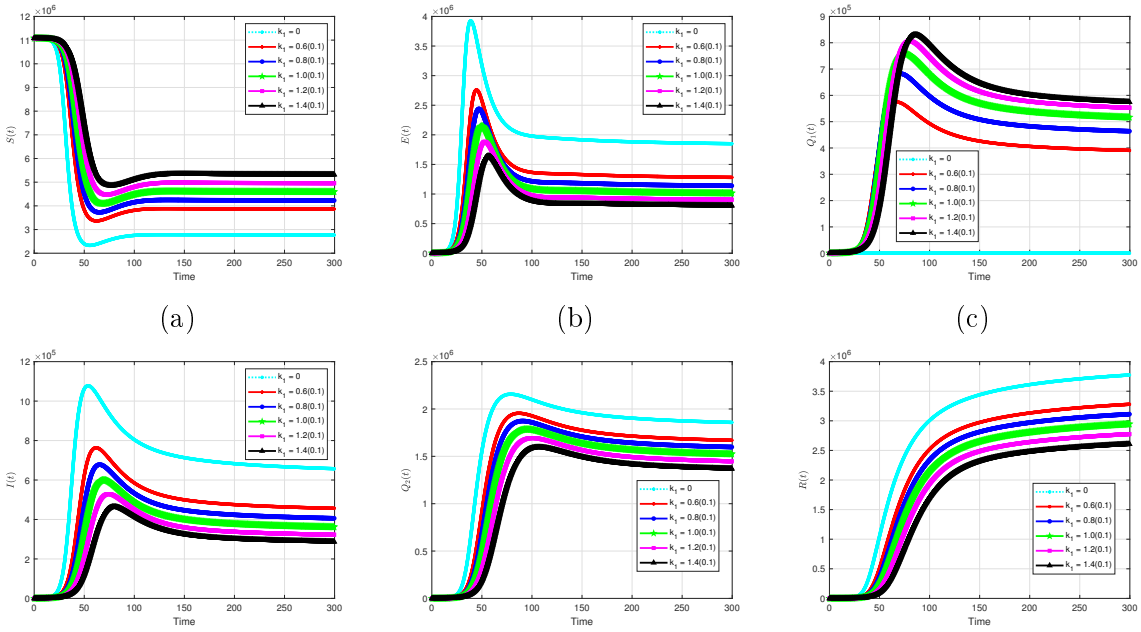

Figure 10: $\alpha = 0.7$ with different k_1

We ran simulations of the model to access the population-level impact of quarantining on the outbreak. The simulations results are displayed in Figures 7 (a) – (f), for $\alpha = 1$. The results for $\alpha = 0.9$, $\alpha = 0.8$, $\alpha = 0.7$ are given in Figure 8 (a) – (f), Figure 9 (a) – (f), Figure 10 (a) – (f), respectively. The results show that quarantining exposed individuals reduces the number of infected individuals. For example, the default scenario result, with $\alpha = 1$, shows a projected 800000 cases at the peak time (Figure 7 (a)).

Preprints (www.preprints.org) | NOT PEER-REVIEWED | Posted: 2 April 2021 doi:10.20944/preprints202104.0052.v1

Without quarantining, about 1400000 cases will be recorded at the peak time. This result is approximately a 75% increment of cases. A 40% increase in quarantine baseline value results in approximately a 25% (600000) reduction in infected cases, Figure 7 (a). Similarly, with the default value $k_1 = 0.1$, the projected peak daily infected cases was 700000 observed for $\alpha = 0.9$, 625000 cases reached for $\alpha = 0.8$, and 600000 cases attained for $\alpha = 0.7$. A 40% increase in quarantining rate from the baseline value results in about $20\% - 25\%$ reduction of infected cases, Figures 8 (d), 9 (d), 10 (d).

5.2.4 The impact of the loss of immunity

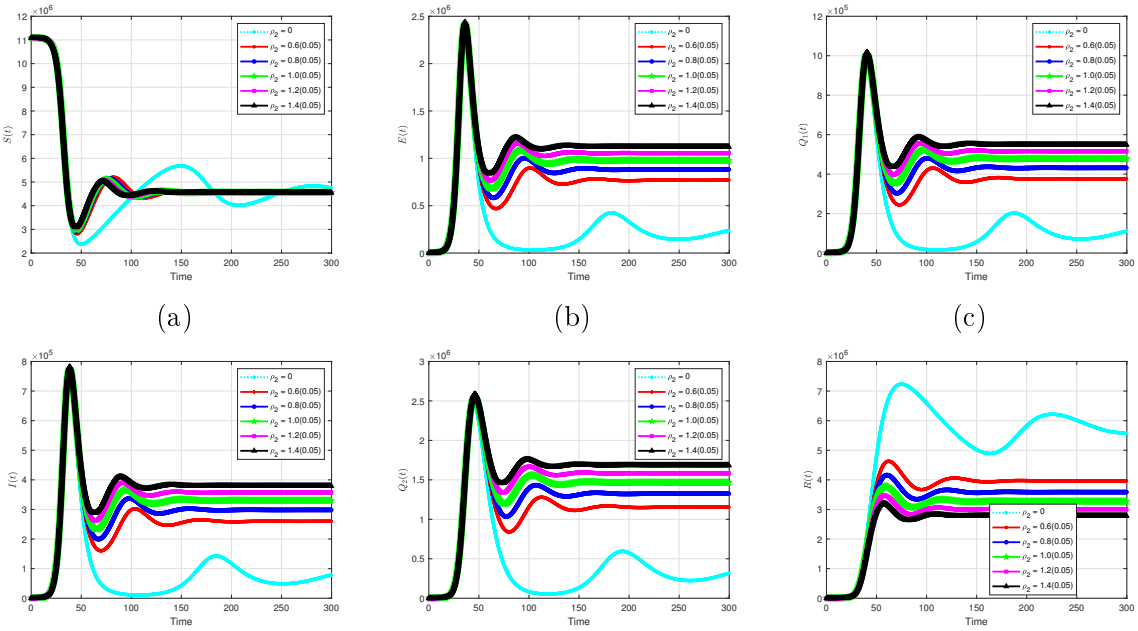

(a) (b) (c)

(d) (e) (f)

Figure 11: $\alpha = 1$ with different ρ_2

Preprints (www.preprints.org) | NOT PEER-REVIEWED | Posted: 2 April 2021 doi:10.20944/preprints202104.0052.v1

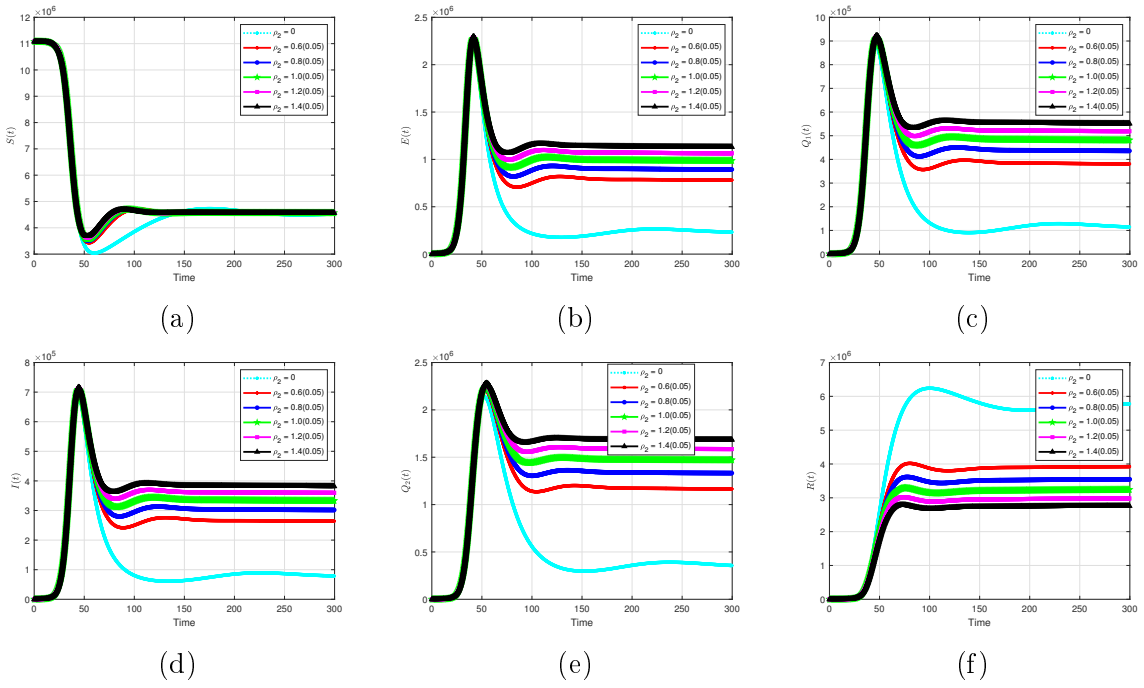

(a) (b) (c)

(d) (e) (f)

Figure 12: $\alpha = 0.9$ with different ρ_2

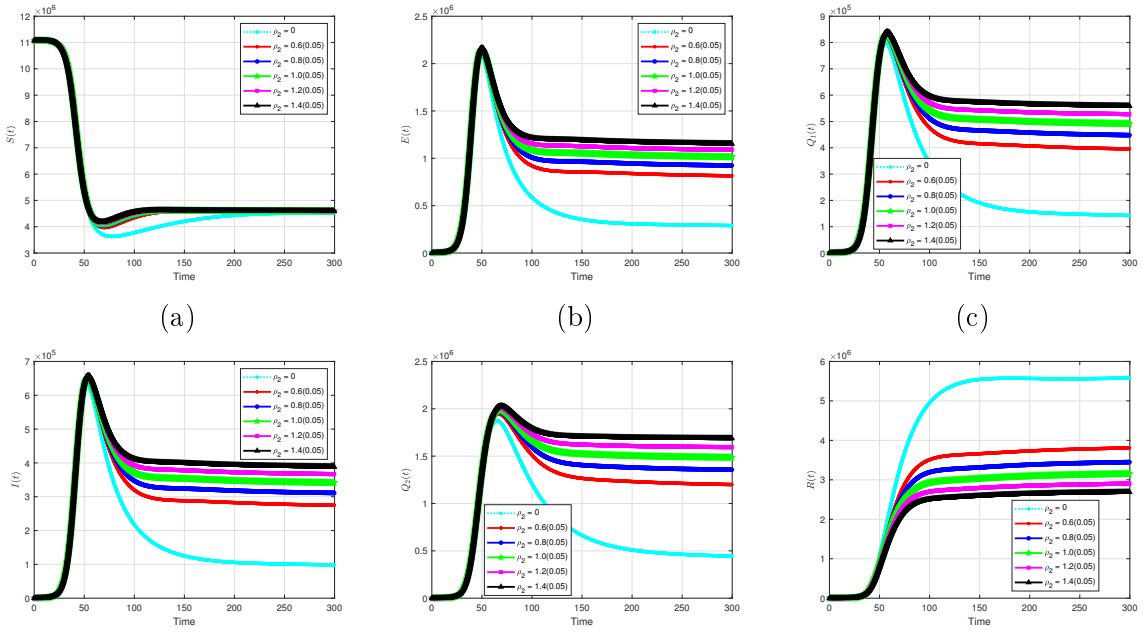

(a) (b) (c)

(d) (e) (f)

Figure 13: $\alpha = 0.8$ with different ρ_2

Preprints (www.preprints.org) | NOT PEER-REVIEWED | Posted: 2 April 2021 doi:10.20944/preprints202104.0052.v1

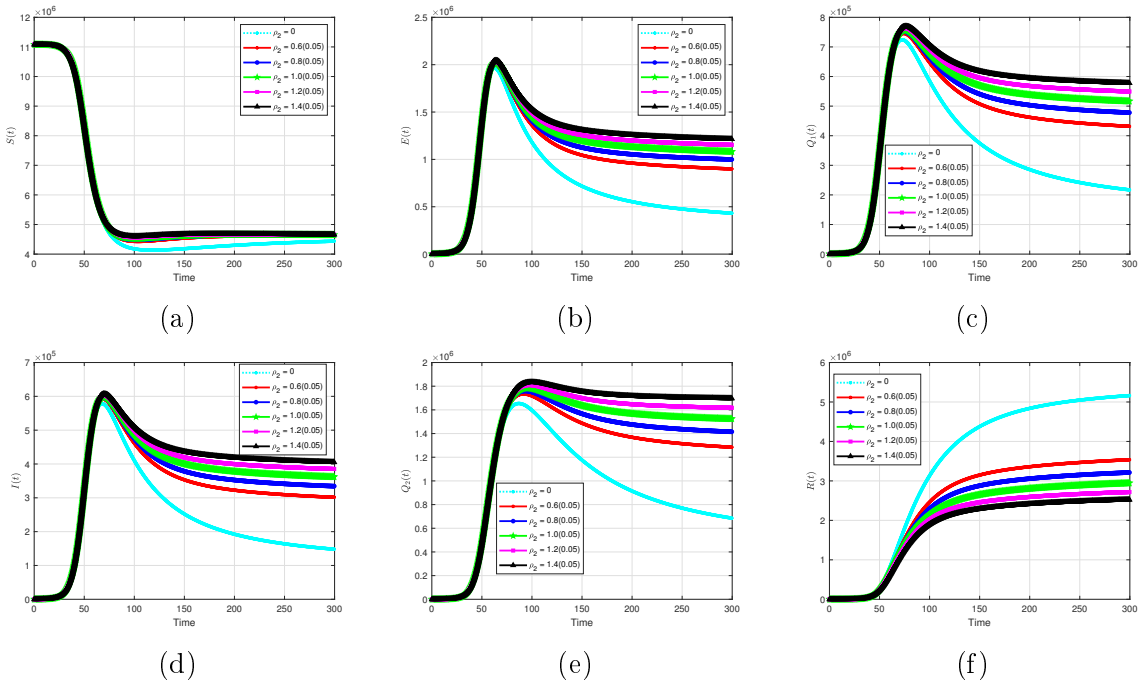

Figure 14: $\alpha = 0.7$ with different ρ_2

There are several reports of re-infection of the COVID-19 cases. We simulated and investigated the impacts of transition rate from recovered to susceptible individuals (loss of immunity) on the dynamics of the solution profiles. The results are displayed in Figures 11 (a)- (f), 12 (a)- (f), 13 (a)- (f), and 14 (a)- (f). We observed that loss of immunity increases the number of infected cases. Without it, the number of individuals in the recovered compartment rises.

Preprints (www.preprints.org) | NOT PEER-REVIEWED | Posted: 2 April 2021 doi:10.20944/preprints202104.0052.v1

5.2.5 The impact of quarantine infected individuals on the solution profiles for the COIVD-19 model

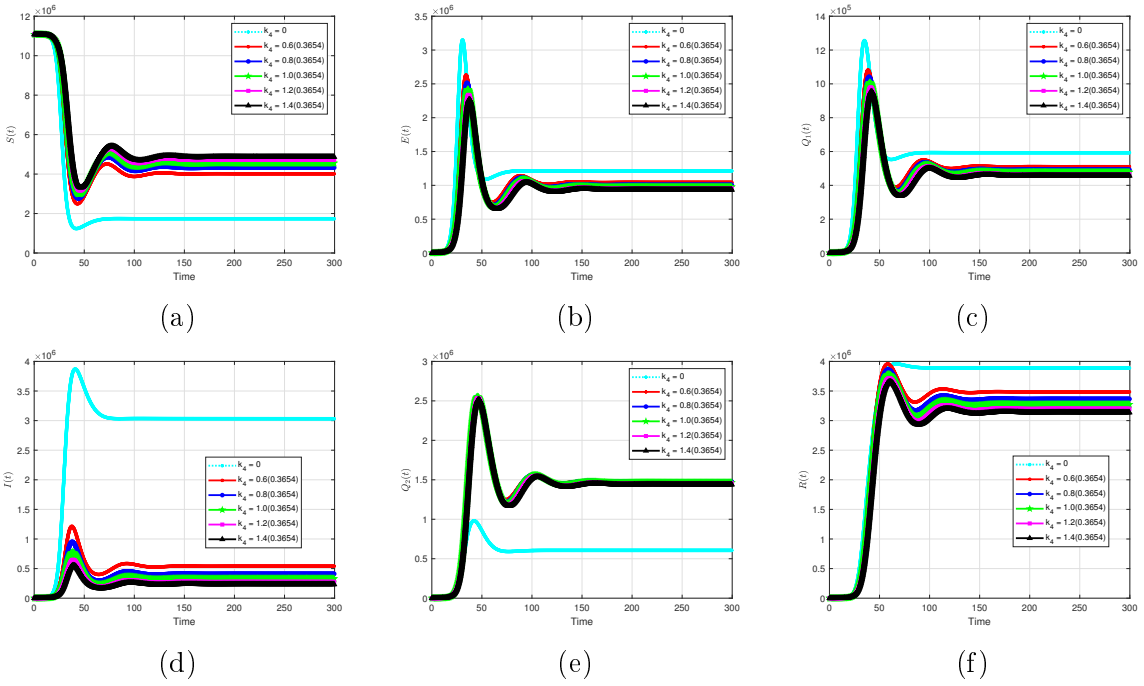

Figure 15: $\alpha = 1$ with different k_4

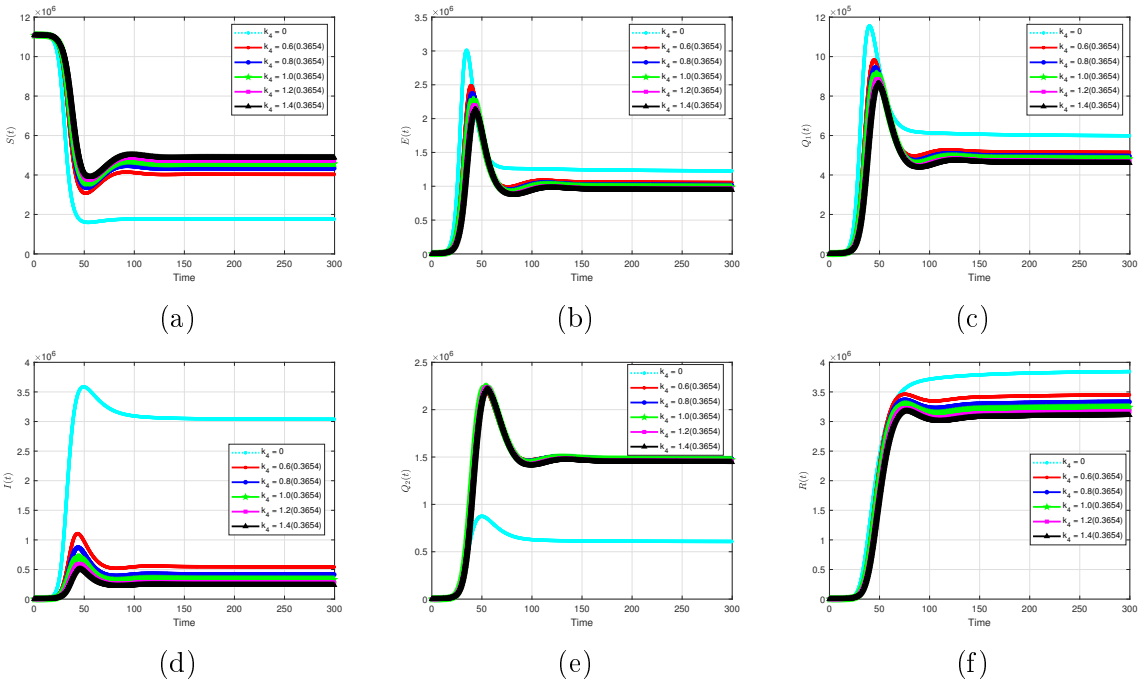

Figure 16: $\alpha = 0.9$ with different k_4

Preprints (www.preprints.org) | NOT PEER-REVIEWED | Posted: 2 April 2021 doi:10.20944/preprints202104.0052.v1

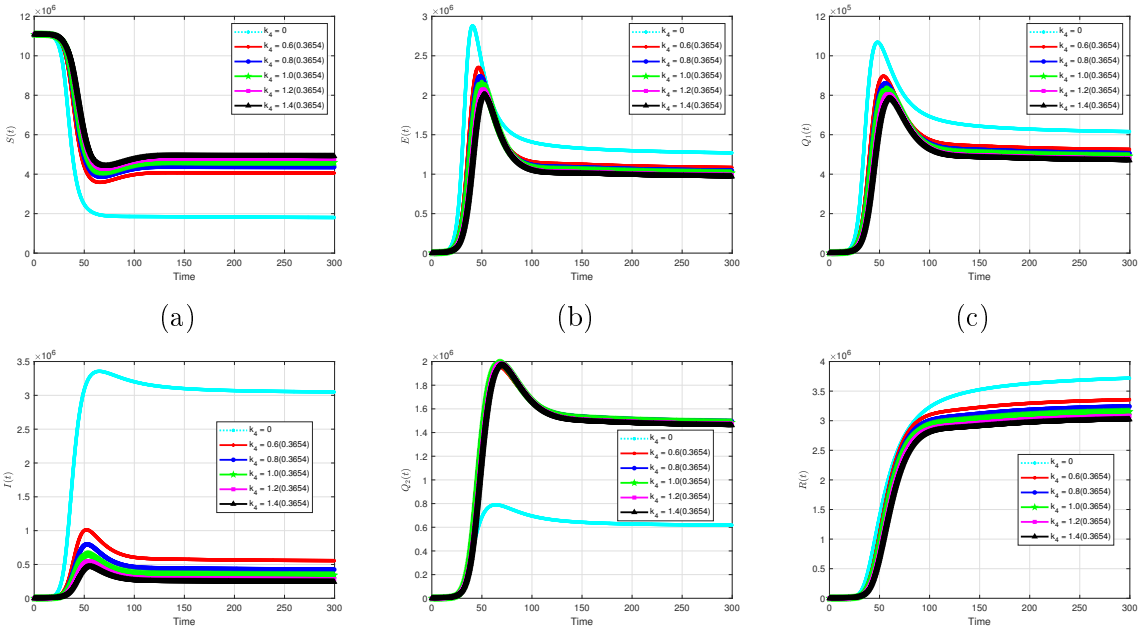

Figure 17: $\alpha = 0.8$ with different k_4

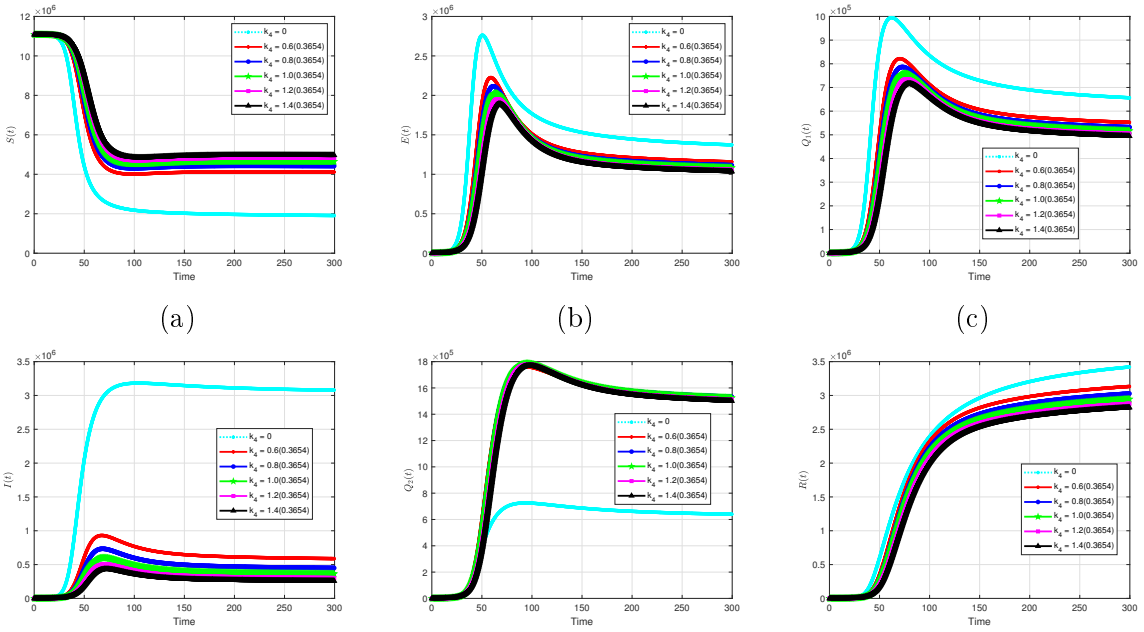

Figure 18: $\alpha = 0.7$ with different k_4

The impact of quarantining infected individuals was also investigated. The simulation results for different k_4 are given in Figure 15 (a) – (f) for $\alpha = 1$, Figure 16 (a) – (f) for $\alpha = 0.9$, Figure 17 (a) – (f), for $\alpha = 0.8$, and Figure 18 (a) – (f) for $\alpha = 0.7$. The results indicate that a high quarantining rate decreases the number of individuals in the infected (I) and exposed (E) classes. As displayed in Figures 15 (b), (d), 16 (b), (d), 17 (b), (d), without quarantine intervention, the exposed and infected populations grow faster with

 doi:10.20944/preprints202104.0052.v1

very high peak levels. In Figure 15 (d), with a 40% increase in quarantining rate from the baseline value, about 50000 cases are observed at the peak time. Without quarantine, approximately 3800000 people will be infected at the peak time; thus, over 400% increase of infected cases.

6 Conclusion

The COVID-19 spread has caused many damages, and it is still posing a significant challenge to individuals and countries. Many studies have been conducted to understand the transmission dynamics and control of the outbreak. The complexity of the disease is very high, and the rate at which it spreads is alarming. Based on this, we have proposed a fractional SEQIR model that captured many intrinsic properties of the transmission of the virus (COVID-19). Deep and extensive simulations in this paper provided insights and exposed hidden properties in the transmission of the coronavirus.

The proposed generalized compartmental COVID-19 model incorporates many key parameters to gain insight into the complexity of the disease. Effective contact rate, transition rate (from exposed quarantine and recovered to susceptible and infected quarantined individuals), quarantine rate, disease-induced death rate, natural death rate, natural recovery rate, and recovery rate of quarantine infected are part of our study. We simulated and discussed the parameters on the dynamics of the solution profiles. Detailed analysis of the proposed model was done, and the results on the existence and uniqueness of solutions, local and global stability analysis of the disease-free equilibrium, and sensitivity analysis are rigorously proven. An expression for the reproduction number, the threshold that measures the contagiousness of the outbreak, was established. For numerical solution, we employed the generalized Adam-Bashforth-Moulton method developed for fractional-order model. The effects of the key parameters are also discussed in detail.

Based on the results, quarantining exposed and infected individuals is sensitive and significantly impacts the transmission of the virus. Thus, the importance of quarantine in mitigating the pandemic cannot be overlooked, and an effective strategy to control the spread of the disease. The results also indicate that the effective contact parameter influences the reproduction number and the spread of the disease significantly. We highly recommend using both non-pharmaceutical and pharmaceutical measures to substantially reduce the effective contact rate and minimize the transmission of the virus. New surges in waves have started to occur currently in many places in the world, including the USA. Our results indicate such surges with some appropriate choice of parameters and specific fractional order.

References

[1] World Health Organization (WHO), assessed on June 19, 2020. https://www.who.int/emergencies/diseases/novel-coronavirus-2019/media-resources/news

[2] Iyiola, O.S.; Oduro, B.; Akinyemi, L. *Analysis and solutions of generalized Chagas vectors re-infestation model of fractional order type.* Chaos, Solitons & Fractals, 2021, **145**, 110797.

[3] Lin, Q.; Zhao, S.; Gao, D.; et al. *A conceptual model for the coronavirus disease 2019 (COVID-19) outbreak in Wuhan, China with individual reaction and governmental action.* Int. J. Infectious Diseases, 2020, **93**, 211-216.

[4] Owusu-Mensah, I.; Akinyemi, L.; Oduro, B.; Iyiola, O.S. *A fractional order approach to modeling and simulations of the novel COVID-19.* Advances in Difference Equations, 2020, **1**, 1-21.

[5] Xinmiao, R.; Liu, Y.; Huidi, C.; Meng, F. *Effect of delay in diagnosis on transmission of covid-19.* Mathematical Biosciences and Engineering, 2020, **17** (mbe-17-03-149), 2725.

[6] Fang, Y.; Nie, Y.; Penny, M. *Transmission dynamics of the covid-19 outbreak and effectiveness of government interventions: A data-driven analysis.* J Med Virol., 2020, **92**, 645-659. doi: 10.1002/jmv.25750.

[7] Adeniyi, M.O.; Matthew, I.E.; Iluno, C.; Ogunsanya A.S.; Akinyemi J.A.; Oke, S.I.; Matadi M.B. *Dynamic model of COVID-19 disease with exploratory data analysis.* Scientific African, 2020, **9**, e00477.

[8] Anastassopoulou, C.; Russo, L.; Tsakris, A.; Siettos, C. *Data-based analysis, modelling and forecasting of the COVID-19 outbreak.* PLoS One, 2020, **15**, 1-21. https://doi.org/10.1371/journal.pone.0230405

[9] Oke, S.I.; Ojo, M.M.; Adeniyi, M.O.; Matadi, M.B. *Mathematical modeling of malaria disease with control strategy.* Commun. Math. Biol. Neurosci., 2020, 43.

[10] Okedoye, A.M.; Salawu, S.O.; Oke, S.I.; Oladejo, N.K. *Mathematical analysis of affinity hemodialysis on T-Cell depletion.* Scientific African, 2020, e00427.

[11] Gbadamosi, B.; Ojo, M.M.; Oke, S.I.; Matadi, M.B. *Qualitative analysis of a Dengue fever model.* Mathematical and Computational Applications, 2018, **23**(3),

[12] Kumar, D.; Seadawy, A.R.; Joardar, A.K. *Modified Kudryashov method via new exact solutions for some conformable fractional differential equations arising in mathematical biology.* Chin. J. Phys., 2018, **56**(1), 75-85.

[13] Iyiola O.S.; Zaman F.D.: A fractional diffusion equation model for cancer tumor. American Institute of Physics Advances, 2014, 4:107121.

[14] Baleanu, D., Wu, G.C., Zeng, S.D.: Chaos analysis and asymptotic stability of generalized Caputo fractional differential equations. Chaos, Solitons Fract., 2017, **102**, 99-105.

[15] Nasrolahpour, H.: A note on fractional electrodynamics. Commun. Nonlinear. Sci. Numer. Simul., 2013, **18**, 2589-2593.

[16] Hilfer, R., Anton, L.: Fractional master equations and fractal time random walks. Physical Review E, 1995, **51**, R848-R851.

[17] Zhang, Y., Pu, Y.F., Hu, J.R., Zhou, J.L.: A class of fractional-order variational image in-painting models. Appl. Math. Inf. Sci., 2012, **6**(2), 299-306.

[18] Pu, Y.F.: Fractional differential analysis for texture of digital image. J. Alg. Comput. Technol., 2007, **1**(3), 357-380.

[19] Baleanu, D., Guvenc, Z.B., Machado, J.T.: New Trends in Nanotechnology and Fractional Calculus Applications. Springer, 2010.

[20] Mainardi, F.: Fractional Calculus and Waves in Linear Viscoelasticity. Imperial College Press, 2010.

[21] Tarasov, V.E., Tarasova, V.V.: Time-dependent fractional dynamics with memory in quantum and economic physics. Ann. Phys., 2017, **383**, 579-599.

[22] Sun, H.G., Zhang, Y., Baleanu, D., Chen, W., Chen, Y.Q.: A new collection of real world applications of fractional calculus in science and engineering. Commun. in Nonlinear. Sci. Numer. Simulat., **64**, 213-231.

[23] Senol M. Analytical and approximate solutions of (2+1)-dimensional time-fractional Burgers-Kadomtsev-Petviashvili equation. Commun Theor Phy., 2020, 72(5), 1-11.

[24] Akinyemi L, Iyiola O.S. *Exact and approximate solutions of time-fractional models arising from physics via Shehu transform.* Math Meth Appl Sci., 2020, 1-23. https://doi.org/10.1002/mma.6484

[25] Akinyemi L, Iyiola O.S. *A reliable technique to study nonlinear time-fractional coupled Korteweg-de Vries equations.* Adv Differ Equ., 2020, 169,1-27. https://doi.org/10.1186/s13662-020-02625-w

[26] Akinyemi L. *q-Homotopy analysis method for solving the seventh-order time-fractional Lax's Korteweg–de Vries and Sawada–Kotera equations.* Comp Appl Math., 2019, 38(4), 1-22.

[27] Şenol M.; Iyiola O.S.; Daei Kasmaei H.; Akinyemi L. *Efficient analytical techniques for solving time-fractional nonlinear coupled Jaulent-Miodek system with energy-dependent Schrödinger potential.* Adv Differ Equ., 2019, 1-21.

[28] Akinyemi L.; Iyiola O.S.; Akpan U. *Iterative methods for solving fourth- and sixth order time-fractional Cahn-Hillard equation.* Math Meth Appl Sci., 2020, 43(7), 4050-4074. https://doi.org/10.1002/mma.6173

[29] Iyiola O.S. *Exact and Approximate Solutions of Fractional Diffusion Equations with Fractional Reaction Terms.* Progr Fract Differ Appl., 2016, 2(1), 21-30.

[30] Iyiola O.S. *On the solutions of nonlinear time-fractional gas dynamic equations: an analytical approach.* Int J Pure Appl Math., 2015, 98(4), 491-502.

[31] Podlubny, I. *Fractional Differential Equations.* Vol. 198 of Mathematics in Science and Engineering, Academic Press, San Diego, Calif, USA, 1999.

[32] Prabhakar, T.R. *A singular integral equation with a generalized mittag-leffler function in the kernel.* Yokohama Math. J., 1971, 19, 7-15.

[33] Iyiola, O.S.; Asante-Asamani, E.O.; Wade, B.A. *A real distinct poles rational approximation of generalized Mittag-Leffler functions and their inverses: Applications to fractional calculus.* Journal of Computational and Applied Mathematics, 2018, 330, 307-317.

[34] Furati, K.M.; Iyiola, O.S.; Mustapha, K. *An inverse source problem for a two-parameter anomalous diffusion with local time datum* Computers and Mathematics with Applications, 2017, 73, 1008-1015.

[35] Odibat, Z.M.; Shawagfeh, N.T. *Generalized Taylor's formula.* Applied Mathematics and Computation, 2007, 186, 286-293.

[36] World Health Organization. WHO COVID-19 Dashboard: https://who.sprinklr.com. Retrieved 7th April, 2020.

[37] CDC: Coronavirus Disease 2019 (COVID-19) Underlying Health Conditions: https://www.cdc.gov/coronavirus/2019-ncov/hcp/underlying-conditions.html Retrieved 6th April, 2020.

[38] Tang, B.; Bragazzi, N.L.; Li, Q.; Tang, S.; Xiao, Y.; Wu, J. *An updated estimation of the risk of transmission of the novel coronavirus (2019-nCov).* Infectious Disease Modelling, 2020, 5, 248-255.

[39] Rong, X.; Yang, L.; Chu, H.; Fan, M. *Effect of delay in diagnosis on transmission of COVID-19.* MBE, 17(3), 2725-2740. DOI: 10.3934/mbe.2020149.

[40] Lauer, S. A.; Grantz, K. H.; Bi, Q.; Jones, F.K.; Zheng, Q.; Meredith, H. R.; ... & Lessler, J. *The incubation period of coronavirus disease 2019 (COVID-19) from publicly reported confirmed cases: estimation and application.* Annals of internal medicine. ePub ahead of print, 2020.

[41] Li, R.; Pei, S.; Chen, B.; Song, Y.; Zhang, T.; Yang, W.; & Shaman, J. *Substantial undocumented infection facilitates the rapid dissemination of novel coronavirus (SARS-CoV2).* Science. 2020.

[42] Liu, T.; Hu, J.X.; Kang, M.; Lin, L.; Zhong, H.; Xiao, J.; et al. *Transmission dynamics of 2019 novel coronavirus (2019-nCoV). bioRxiv*, 2020.

[43] Zhou, F.; Yu, T.; Du, R.; Fan, G.; Liu, Y.; Liu, Z.; ... & Guan, L. *Clinical course and risk factors for mortality of adult inpatients with COVID-19 in Wuhan, China: a retrospective cohort study.* The Lancet. 2020.

[44] Huang, C.; Wang, Y.; Li, X.; Ren, L.; Zhao, J.; Hu, Y.; et al., *Clinical features of patients infected with 2019 novel coronavirus in Wuhan, China.* Lancet, 2020, 395, 497-506.

[45] Lin, W., Global existence theory and chaos control of fractional differential equations, Journal of Mathematical Analysis and Applications 332 (2007) 709-726.

[46] Keeling, M.J.; Rohani, P. *Modeling Infectious diseases in Humans and Animals. Princeton Univ. Press.* 2008.

[47] Diekmann, O.; Heesterbeek, J.A.P.; Britton, T. *Mathematical Tools for Understanding Infectious Disease Dynamics. Kindle Edition.* Princeton University Press.

[48] Driessche, P.V., Watmough, J. *Reproduction numbers and sub-threshold endemic equilibria for compartmental models of disease transmission. Mathematical Biosciences*, 2002, **180**, 29–48.

[49] Heesterbeek, J.A.P. *A brief history of R0 and a recipe for its calculation. Acta Biotheo*, 2002, **50**, 189–204.

[50] Gumel A.B.; Lubuma J.M.; Sharomi O.; Terefe Y.A. *Mathematics of a sex-structured model for syphilis transmission dynamics.* Math Meth Appl Sci., 2017, 1-26. DOI: 10.1002/mma.4734

[51] Suryanto, A.; Darti, I.; Panigoro, H.S.; Kilicman, A. *A fractional-order predator-prey model with ratio-dependent functional response and linear harvesting.* Mathematics, 2019, 7, 1100, doi:10.3390/math7111100.

[52] Chitnis, N.; Hyman, J.M.; Cushing, J.M. *Determining important parameters in the spread of malaria through the sensitivity analysis of a mathematical model.* Bulletin of Mathematical Biology, 2008, 70, 1272–1296. doi:10.1007/s11538-008-9299-0.

[53] Okosun K.O.; Rachid O.; Marcus N. *Optimal control strategies and cost-effectiveness analysis of a malaria model.* BioSystems. 2013, 111, 83–101.

[54] Oduro, B.; Apenteng, O.O.; Nkansah, H. *Assessing the effect of fungicide treatment on Cocoa black pod disease in Ghana: Insight from mathematical modeling. Statistics.* Optimization & Information Computing, 2020. https://doi.org/10.19139/soic-2310-5070-686

[55] Ndairou, F.; Area, I.; Nieto, J.J.; Torres, D.F.M. *Mathematical Modeling of COVID-19 Transmission Dynamics with a Case Study of Wuhan.* Chaos, Solitons and Fractals, 2020. doi: https://doi.org/10.1016/j.chaos.2020.109846

[56] Diethelm, K.; Freed, A.D. *The FracPECE subroutine for the numerical solution of differential equations of fractional order*, in: S. Heinzel, T. Plesser (Eds.), Forschung und Wissenschaftliches Rechnen 1998, Gessellschaft fur Wissenschaftliche Datenverarbeitung, Gottingen, 1999, pp. 57-71.

[57] Diethelm, K.; Ford,N.J.; Freed, A.D. *A Predictor-Corrector Approach for the Numerical Solution of Fractional Differential Equations.* Nonlinear Dynamics 2002, 29, 3-22.

[58] Garrappa, R. *On linear stability of predictor-corrector algorithms for fractional differential equations.* Internat. J. Comput. Math., 2010, 87(10), 2281-2290.

[59] Garrappa, R. *Predictor-corrector PECE method for fractional differential equations* (https://www.mathworks.com/matlabcentral/fileexchange/32918-predictor-corrector-pece-method-for-fractional-differential-equations), MATLAB Central File Exchange. Retrieved May 14, 2020.